The role of DAF-41 in lifespan of Caenorhabditis elegans

Sačer, Margareta

Master's thesis / Diplomski rad

2024

Degree Grantor / Ustanova koja je dodijelila akademski / stručni stupanj: **University of Zagreb, Faculty of Science / Sveučilište u Zagrebu, Prirodoslovno-matematički fakultet**

Permanent link / Trajna poveznica: https://urn.nsk.hr/urn:nbn:hr:217:564872

Download date / Datum preuzimanja: **2025-03-04**

Repository / Repozitorij:

Repository of the Faculty of Science - University of Zagreb

Sveučilište u Zagrebu
Prirodoslovno-matematički fakultet
Biološki odsjek

Margareta Sačer

Uloga proteina DAF-41 u životnom vijeku
Caenorhabditis elegans

Diplomski rad

Zagreb, 2024.

University of Zagreb

Faculty of Science

Department of Biology

Margareta Sačer

The Role of DAF-41 in Lifespan of

Caenorhabditis elegans

Master thesis

Zagreb, 2024.

Acknowledgments

TEMELJNA DOKUMENTACIJSKA KARTICA

Uloga proteina DAF-41 u životnom vijeku

Caenorhabditis elegans

Margareta Sačer

Rooseveltov trg 6, 10000 Zagreb, Hrvatska

Tiku i suradnici (2017) primijetili su da delecija gena tumor-supresora NCL-1 (eng. *Nucleoli 1*) skraćuje produljeni životni vijek u više dugovječnih modela *Caenorhabditis elegans*, među kojima i u dvostrukom mutantu *glp-1ncl-1* (eng. *Abnormal Germ Line Proliferation* 1). Prethodno neobjavljena istraživanja Antebija i suradnika nedavno su identificirala protein DAF-41 (eng. *Abnormal Dauer Formation 41*), ko-šaperon proteina HSP-90 (eng. *Heat Shock Protein 90*) kao potencijalnog nizvodnog regulatora životnog vijeka mutanta *glp-1ncl-1*. Otkrila sam da utišavanje gena *daf-41* produžuje životni vijek *C. elegans* mutanta *glp-1ncl-1*. Kako bih otkrila potencijalni signalni put ovog fenomena, provela sam RT-qPCR analizu gena inzulinskog signalnog puta (*daf-16, lipl-4, sod-3, dod-3*), odgovora na toplinski šok (*hsf-1, hsp-70, hsp-16.2, hsp-4*) i steroidnog signalnog puta (*daf-12, fard-1, cdr-6, daf-36*). Zatim sam kvantificirala aktivnost fluorescentno obilježenih transkripcijskih faktora HSF-1 i DAF-16 te mjerila otpornost oblića na toplinski i oksidativni stres. Međutim, promjene u ekspresiji gena, aktivnosti DAF-16 i HSF-1, otpornost na toplinski i oksidativni stres nisu dali jasan uvid u mehanizam produženja životnog vijeka mutanata *glp-1ncl-1* s utišanim genom *daf-41*.

BASIC DOCUMENTATION CARD

University of Zagreb
Faculty of Science
Department of Biology   Master thesis

The Role of DAF-41 in Lifespan of *Caenorhabditis elegans*

Margareta Sačer

Rooseveltov trg 6, 10000 Zagreb, Croatia

Tiku et al. (2017) published that loss of the protein NCL-1 (abnormal NuCLeoli 1) abolishes the extended lifespan in major *Caenorhabditis elegans* longevity pathways, including the germline-deficient *glp-1* (abnormal Germ Line Proliferation 1) *C. elegans* mutant. Recent unpublished work from the Antebi group identified a protein DAF-41 (Abnormal Dauer Formation 41), an HSP-90 (heat shock protein 90) co-chaperone, as a potential downstream regulator of *glp-1ncl-1* lifespan. I investigated the role of *daf-41* in *glp-1ncl-1* lifespan, finding that *daf-41* downregulation extended the lifespan of *glp-1ncl-1* worms. Moreover, I performed RT-qPCR analysis of genes associated with the insulin signaling pathway (*daf-16, lipl-4, sod-3, dod-3*), heat-shock response (*hsf-1, hsp-70, hsp-16.2, hsp-4*), and steroid pathway (*daf-12, fard-1, cdr-6, daf-36*), quantified GFP-tagged HSF-1 and DAF-16 transcription factor activity and measured thermotolerance and oxidative stress resistance in different mutant backgrounds. Changes in gene expression, DAF-16 and HSF-1 activity, thermotolerance, and oxidative stress resistance did not clearly explain the mechanism behind this lifespan extension.

Table of Contents

Abbreviations

age-1 - AGEing alteration 1

AKT-1/2 - AKT Serine/Threonine Kinase

AMPK - Adenosine Monophosphate Kinase

cDNA – Complementary DNA

cdr-6 - Cadmium Responsive 6

clk-1 - CLocK (biological timing) abnormality

C_t - cycle threshold

C. elegans - Caenorhabditis elegans

DA - dafachronic acid

daf-2 - abnormal DAuer Formation 2

daf-9 - abnormal DAuer Formation 9

daf-12 - abnormal DAuer Formation 12

daf-16- abnormal DAuer Formation 16

daf-36 - abnormal DAuer Formation 36

daf-41 - DAuer Formation 41

DIC - Differential Interference Contrast

DNA - DeoxyriboNucleic Acid

DNC - Dorsal Nerve Cord

dod-3 - downstream of *daf-16*

DR - Dietary Restriction

dsRNA – Double-Stranded RNA

eat-2 - EATing: abnormal pharyngeal pumping 2

[ER]UPR - Unfolded Protein Response of Endoplasmic Reticulum

E. coli – Escherichia coli

fard-1 - Fatty Acyl-CoA ReDuctase 1

FIB-1 - FIBrillarin family

FOXO - human FOrkhead boX O

FUdR - 5'-Fluorodeoxy Uridine

GFP - Green Fluorescent Protein

glp-1 - abnormal Germ Line Proliferation 1

HLH-30/TFEB - Helix Loop Helix, an ortholog of the mammalian Transcription Factor EB

HSF-1 - Heat Shock Factor 1

HSP - Heat Shock Protein

IGF-1 - Insulin Growth Factor

IIS - insulin/IGF-1 signalling

JNK - Janus kinase

L1, L2, L3, L4 – larval 1, 2, 3, 4

L3d - L3 Dauer

LBP-8 - Lipid Binding Protein 8

let-363 - LEThal 363

LG - Linkage Groups

lipl-4 – LIPase 4

luci - LUCIferase

Mb - MegaBase

mir-81- MIcRo-RNA 81

mir-241 MIcRo-RNA 241

mRNA – Messenger RNA

mTOR - Mammalian Target Of Rapamycin

n – the Number of biological replicates

N – the Number of worms

ncl-1 - abnormal NuCLeoli 1

NFE2 - Nuclear Factor, Erythroid 2

NHR-49 - Nuclear Hormone Receptor 49

NHR-80 - Nuclear Hormone Receptor 80

NRF2 - NFE2-related factor

PDK-1 - Phosphoinositide-Dependent protein Kinase-1

PFKL - PhosphoFructoKinase

PGE2 – ProstaGlandin E2

PI3K - PhosphoInositide 3 Kinase

PIP3 - PhosphatidylInositol-3,4,5-triPhosphate

PTGES3 - ProsTaGlandin E2 Synthase 3

raga-1 - RAs-related GTP-binding protein A

RNA - RiboNucleic Acid

RNAi - RNA interference

RNase - RiboNucleASE

ROS - Reactive Oxygen Species

rRNA – Ribosomal RNA

RT-qPCR - Quantitative Reverse Transcription Polymerase Chain Reaction

SKN-1 – SkiNhead 1

snb-1 - SyNaptoBrevin related

sod-3 - SuperOxide Dismutase 3

TF - Transcription Factor

TGF-β - Transforming Growth Factor Beta

TORC1 – Target of Rapamycin Complex 1

TRIM2 - Tripartite Motif Containing 2

VNC - Ventral Nerve Cord

1. Introduction

1.1. Basic Features of *Caenorhabditis elegans*

Caenorhabditis elegans is a well-known and widely used research animal model due to the ease and low cost of maintenance, well-defined anatomy, short generation time, fully sequenced genome and the ability to self-fertilize.

1.1.1. Morphology and Anatomy

In nature, *C. elegans* is usually found as a 1 mm long, free-living soil nematode feeding on bacteria. Although it belongs to the phylum of Nematoda, *C. elegans* is referred to as a worm in the literature. In the English language it is an expression common for all invertebrates with the worm-like body shape. For this reason, from now on, I will be referring to *C. elegans* as a worm. Due to its small size, it is difficult to isolate tissues and organs, but its transparent cylindrical body helps to define its anatomy. Body wall muscle is innervated with dorsal and ventral nerve cords connected via nerve ring in the head region, while the digestive system, which starts with the mouth, continues with the pharynx and intestine and ends with the anus at the tail. Hermaphrodites' reproductive system alongside gonad and spermatheca, contains many oocytes which, when fertilised, develop into embryos and exit the adult worm through the vulva (Figures 1.A, 1.B) (Corsi et al., 2015a).

One of the major advantages of *C. elegans* as a model is the fact that it has defined tissues and an invariant number of cells. The outermost layer of cells - the epidermis (traditionally called hypodermis) consists of syncytial cells that secrete a protective cuticle. Underneath the epidermis is muscle tissue innervated by the ventral and dorsal nerve cords (VNC = "ventral nerve cord", DNC = "dorsal nerve cord"). Inside, a pseudocoelomic fluid-filled cavity houses

reproductive, digestive and excretory systems (Figure 1.C), along with coelomocytes, cells with a similar function of vertebrate macrophages (Corsi et al., 2015a).
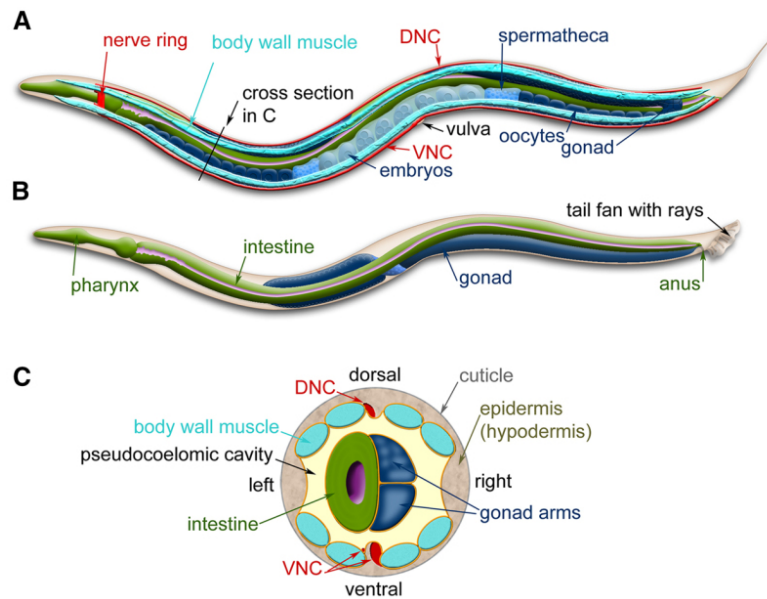
Figure 1. C. elegans hermaphrodite (A) and male (B) anatomy. The body wall muscle is innervated by dorsal and ventral nerve cords, which are connected via a nerve ring in the head region (A). The digestive system starts at the mouth, continues through the pharynx and intestine, and ends at the anus in the tail region (B). In hermaphrodites (A), the reproductive system, which includes the gonad and spermatheca, contains oocytes that, once fertilized, develop into embryos and exit the mother through the vulva. The position of a cross section shown in (C) is indicated by a black line in (A). The epidermis (hypodermis) is composed of syncytial cells that secrete the cuticle. Beneath the epidermis lies muscle tissue, which is innervated by the ventral and dorsal nerve cords (VNC = "ventral nerve cord", DNC = "dorsal nerve cord"). Inside, a pseudocoelomic fluid-filled cavity houses the reproductive, digestive, and excretory systems. This image was generated by Corsi et al. (2015).

1.1.2. Life Cycle and Reproduction

Most of the *C. elegans* population is hermaphrodite as males make up only 0.1-0.2% of hermaphrodite worm progeny. Hermaphrodites are defined by two X chromosomes XX, while males by a single X chromosome X0. A very useful trait of *C. elegans* in research is the fact that self-fertilisation (oftentimes called selfing) produces a high number (around 300) of genetically unified progeny, and if fertilised by a male (called outcrossing), this number gets up to 1000 progeny worms (50% of which are male). Moreover, as self-fertilisation follows the Mendelian segregation rules, getting the desired genotype becomes much easier and quicker

due to the fast generation turnover (Corsi et al., 2015a). Hermaphrodite oocytes are preferably fertilised by a male sperm, which is useful when researchers cross worms to introduce new gene variants into the population (Ward & Carrel, 1979). The observation that the frequency of male progeny increases under stressful conditions (such as increased heat) is often used to generate male progeny of a desired genotype (Morran et al., 2009).

The rate of *C. elegans* development and growth depends on external temperature. In the laboratory environment, it is usually kept at 20 ºC, so I will briefly summarise the *C. elegans* life cycle at this temperature (Figure 2).
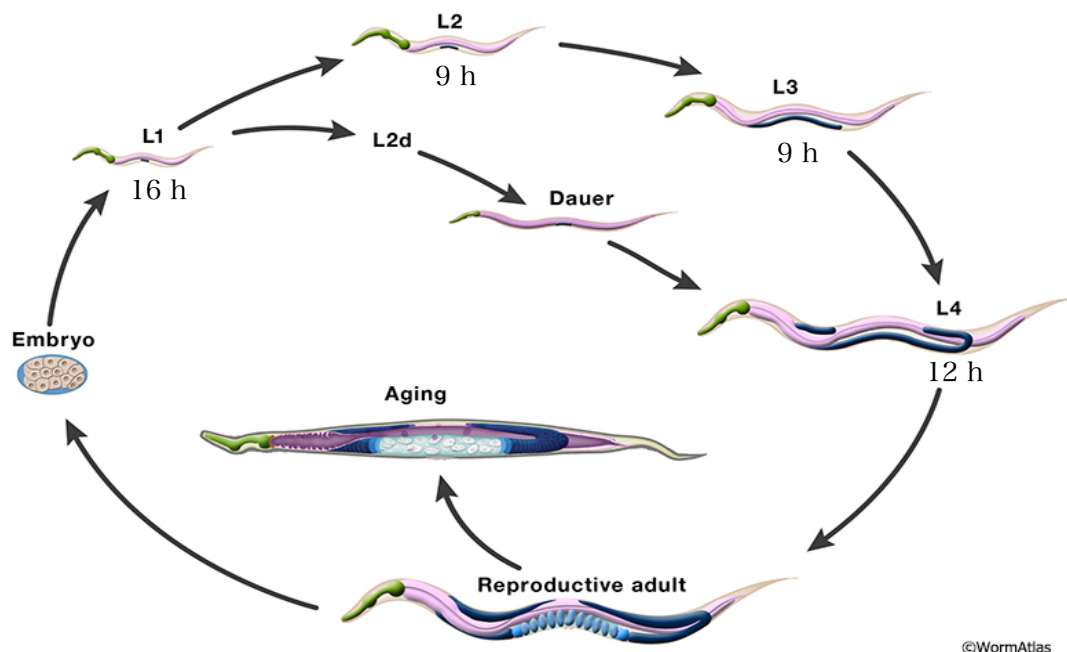
Figure 2. C. elegans life cycle at 20 ºC. After fertilization, an impermeable eggshell forms around the oocyte, and embryos are laid at the 24-cell stage. For the first 16 hours post-hatching, the worms are in the first larval stage, L1. As they feed, they progress through the L2, L3, and L4 stages, each lasting approximately 9-12 hours. Twelve hours after the L4 molt, adult worms begin laying eggs, a process that continues for about three days until they have depleted their sperm cells. The image is based on image by Herndon et al. (2018).

After the oocyte is fertilised, an impermeable eggshell forms and at the 24-cell stage, embryos are laid. For the first 16 hours after hatching, the worms are in the first larval stage - L1. As they feed, they progress into L2, L3 and L4 stages (each lasting approximately 12 hours). Twelve hours after L4 molt, adult worms start laying eggs for approximately three days (unit they have depleted all their sperm cells) (Corsi et al., 2015a).

The rate of growth and progress also depends on the particular genetic strain, which is especially important when maintaining the strain in the laboratory. One should avoid accidentally subjecting the worms to overcrowding and food depletion as L1 larvae enter dauer development and develop into alternative L3d (L3 dauer stage). The Dauer stage is a state of changed physiology meant to protect the worm against an unfavourable environment (Golden & Riddle, 1984). Dauer larvae form an enhanced cuticle that disables eating, arrests development and enables worms to survive for months. If the dauer worms are given food, they continue to develop into L4 stage and then into adults with a slightly changed physiology (Corsi et al., 2015a).

1.1.3. Genome and Genetics

C. elegans was the first multicellular organism to have its genome sequenced (*C. elegans* Sequencing Consortium 1998). The genome is approximately 100 Mb long and has more than 20,000 protein-coding genes (Hodgkin, 2001). The genes are relatively small (on average 3 kb) compared to vertebrate genes due to the small size and lower number of introns and are organised into untranslated regions and open reading frames that contain exons and introns. Both hermaphrodites and males have five autosomal chromosomes I, II, III, IV, and V called linkage groups (LG) and are differentiated by having one (males) or two X chromosomes (hermaphrodites)(Corsi et al., 2015a).

One of the great advantages of this model organism is the fact that approximately 60-80% of all human genes, and 40% of human-disease-associated genes, have a *C. elegans* ortholog (Culetto & Sattelle, 2000; Kaletta & Hengartner, 2006). Besides the previously mentioned advantages of the population mainly being homozygous, genetic manipulation of *C. elegans* is facilitated with RNA (ribonucleic acid) interference (RNAi) by using double-stranded RNA to downregulate gene activity (Fire et al., 1998). The worms are fed with RNase (ribonuclease) III-resistant bacteria (usually *Escherichia coli*) which have high quantities of a desired dsRNA (double-stranded RNA). This, in turn, can produce worms with phenotype corresponding to the gene-downregulated mutant. It is important to note that there is a decreased effectiveness in the nervous system, in early larval stages, and in male worms (Timmons et al., 2001).

1.1.4. Maintenance and Handling in the Laboratory

Due to the small size of *C. elegans*, it is observed and handled under a dissecting or a compound microscope. A dissecting microscope (which allows up to 100x magnification) is used for the observation of *C. elegans* on Petri dishes, while a compound microscope (which allows up to 1000x magnification) is used to observe the animal at a single-cell resolution. As *C. elegans* is transparent, cellular and sub-cellular structures can be observed using differential interference contrast (DIC) optics, while tagged fluorescent proteins can be observed using a particular fluorescent channel (Corsi et al., 2015a). This allows the *in vivo* observation of sub-cellular structures and proteins (Chalfie et al., 1994).

C. elegans is grown on agar Petri dishes (for ease of use, from now called plates) containing a lawn of *E. coli* bacteria as a source of food. Depending on the number of egg-laying adults on a plate and the rate of development (determined by a particular *C. elegans* strain and the maintenance temperature of the incubator), worms are maintained and fed by continuous transfer onto fresh plates before the complete bacteria depletion. This is done either by transferring a few egg-laying adults onto fresh plate, by transferring a chunk of agar-containing worms, or by the bleaching method. It is important not to deplete the worms of food as L1s enter a dauer larval stage which exhibits a changed physiology for the next few generations even after they are fed.

Before performing experiments, the worm population needs to be synchronised at the same life-cycle stage. This is usually done either by the "egg lay method" or by "bleaching". The "egg lay" is performed by allowing a few adult egg-laying worms to lay eggs for up to 3 hours and consequently sacrificing (killing) adults which leaves the plate with several highly synchronous eggs. The "bleaching" method consists of treating adult population of worms with a hypochlorite solution which kills all worms but leaves the eggs inside adults intact (thanks to the resistant eggshell). This leaves the researcher with a slightly less synchronised population compared to the "egg laying method" as an adult carries embryos in different stages of development – from fertilisation until the 24-cell stage. This method is used as a sterilisation method as well, as bleach can eliminate mould and most other common infectants.

Lifespan experiments are often carried out to determine the length of the lifespan in various *C. elegans* conditions. It is usually done one of two ways. The transfer method requires the transfer

of each gravid worm by hand onto a fresh plate every few days to avoid mixing the newly hatched and developed progeny with the experimental worms. The 5'-fluorodeoxyuridine (FUdR) method uses FUdR to sterilise the worms which removes the need to transfer worms onto new plates. Both methods have advantages and disadvantages. Although the transfer method does not influence worm physiology as much as the FUdR method, this method requires increased time and attention and can cause stress to the worms by the fact it is picked multiple times, thus changing its physiology. On the other hand, the FUdR method is much less time-consuming, but it was shown that FUdR changes lifespan in some genotypes through the activation of stress response signalling pathways (Anderson et al., 2016).

Besides the low cost of equipment for maintenance and worm observation, one of the great advantages of *C. elegans* is the ability to freeze any strain of this worm. It can be kept this way for years, shared among researchers and revived when in need (Corsi et al., 2015a)

1.1.5. Nomenclature

Gene names are given and written as lowercase letters followed by a dash and a number, all italicized (example *glp-1*). Transgenic lines containing translational fusion are noted with two colons (example *glp-1::gfp*).

Mutations of the genes are written in the same manner (for example *glp-1*). **Multiple** mutations in the same strain are divided by a semicolon if they are situated on different chromosomes (for example *glp-1;daf-16*). If they are situated on the same chromosome, they are written without a semicolon (for example *glp-1ncl-1*).

Allele names follow the name of the gene and are written in parenthesis (for example *glp-1(e2141ts)*). Wild type allele is indicated with "+". The heterozygous genotype is characterised with a slash (for example *e2141ts/+*).

Gene products - proteins, are written in all capital letters (example GLP-1, GLP-1::GFP). RNAs are written the same as the gene name.

Strain names are written in capital letters and numbers (for example N2). If a strain carries a particular mutation it is written as an italicized mutated gene name, sometimes followed by an italicized name of the chromosome [example *glp-1(e2141)*]. The name of the strain should note

if there is a transcriptional or promotor fusion (for example *mab-5p::gfp* transcriptional fusion). (Corsi et al., 2015)

1.2. Overview of *Caenorhabditis elegans* as a Model Organism for Ageing Studies

C. elegans lifespan is temperature-dependent and when grown at 20 ºC, usually lasts 18-20 days. At higher temperatures, it gets shorter, while at colder temperatures gets a few days longer (Klass, 1977).

Physiological changes associated with ageing in *C. elegans* resemble those present in human ageing, making it an interesting model to study ageing. Anatomical changes associated with ageing in *C. elegans* include deterioration of reproductive system (Pickett et al., 2013), neuronal deterioration (Liu et al., 2013), loss of muscular integrity (Podshivalova et al., 2017), decreased activity and accumulation of auto-fluorescent foci (Chew et al., 2017; Garigan et al., 2002; S. Zhang et al., 2020). On the cellular level, ageing leads to loss of nuclear integrity, mitochondrial fragmentation, increased mitochondrial fusion (Dilberger et al., 2019), reduced activity of the unfolded protein response of endoplasmic reticulum (^{ER}UPR) (Martínez et al., 2017) and in a decreased mRNA (messenger ribonucleic acid) splicing fidelity (Son et al., 2019), amongst others.

A landmark study in 1988 discovered a single-gene mutation of *age-1* (ageing alteration 1) increased *C. elegans* lifespan by 40-60% (Friedman & Johnson, 1988), marking the beginning of the genetic approach to ageing research. This was especially surprising as it was thought many genes contributed to ageing to a very small extent that would not be noticeable by a change in just one gene (Campisi et al., 2019).

1.2.1. The Insulin/IGF-1 Signalling Pathway

age-1 encodes a homolog of mammalian phosphoinositide 3 kinase (PI3K) catalytic subunit and is activated by *daf-2* (abnormal dauer formation 2) - an insulin/IGF-1 (insulin growth factor 1) receptor (S. Zhang et al., 2020). *daf-2* loss, as well, can increase worm lifespan by twice as much as the wildtype (Lin et al., 1997). Active *age-1/PI3K* accumulates phosphatidylinositol-3,4,5-triphosphate (PIP3) and thereby activates PDK-1

(phosphoinositide-dependent protein kinase-1). PDK-1 activates AKT-1/2 (AKT Serine/Threonine Kinase) by phosphorylation which in turn inhibits DAF-16 (a homolog of human forkhead box O [FOXO]) transcription factor (Lazaro-Pena et al., 2022). Mutations within the insulin/IGF-1 signalling (IIS) lead to DAF-16 activation through its translocation into the nucleus where it regulates the expression of downstream targets (including *sod-3* [superoxide dismutase 3], *dod-3* [downstream of *daf-16*], *lipl-4* [lipase 4]) and thereby increasing resistance to various kinds of stress leading to increased longevity (Sun et al., 2017). *sod-3* attenuates damage done by reactive oxygen species (ROS) by catalysing the conversion of superoxide anions into hydrogen peroxide and oxygen (Kim et al., 2022). Then, to avoid H_2O_2 damage and toxicity, *C. elegans* relies on H_2O_2 catalases (Schiffer et al., 2021). Moreover, this mechanism is relevant to *C. elegans'* response to ROS generation induced by paraquat, a broadly used herbicide (Ji et al., 2022).

On the other hand, *lipl-4* is a lysosomal lipase that promotes longevity by inducing nuclear translocation of LBP-8 (lipid binding protein 8, a lysosomal lipid chaperone) activating the nuclear hormone receptors NHR-49 and NHR-80 (nuclear hormone receptor 49 and 80) (Folick et al., 2015).

DAF-16 is a key longevity mediator that integrates signals from various signalling pathways, such as nutrient sensing-related mTOR (mammalian target of rapamycin) signalling, germline signalling, or oxidative stress-related JNK (Janus kinase) signalling (Sun et al., 2017). For instance, ROS regulate DAF-16 nuclear import (Putker et al., 2013). Furthermore, dietary restriction promotes longevity through AMPK-mediated (Adenosine monophosphate kinase) activation of DAF-16 (S. Zhang et al., 2020).

Alongside DAF-16, reduced insulin/IGF-1 signalling and oxidative stress promote *C. elegans* longevity through the transcription factor SKN-1 (skinhead 1), the ortholog of the mammalian NFE2-related (nuclear factor erythroid 2) factor (S. Zhang et al., 2020).

1.2.2. Heat Shock Response

The heat shock transcription factor HSF-1 (HSF1 in mammals) plays an important role in increasing the expression of chaperones (HSP-90 [Heat Shock Protein 90], HSP-70, HSP-60, HSP-16.2, HSP-4, among others) in response to various metabolic signals and multiple stressors (heat, oxidative stress) by preserving proteome homeostasis and maintaining proper

protein folding (Lazaro-Pena et al., 2022). It acts within neurons to maintain proteostasis in distal tissues through serotonin signalling (Tatum et al., 2015). Under homeostatic conditions, HSPs are coupled to translation by mediating *de novo* protein folding, while stress induces HSP70 and HSP90 chaperons to reduce protein misfolding (Lazaro-Pena et al., 2022). Upon heat stress, HSF-1 monomers form trimers and trigger subsequent chaperone transcription, but also increase thermotolerance through the maintenance of cytoskeletal integrity (Denzel et al., 2019). In *C. elegans* and mammals, this is followed by the formation of stress granules (HSF-1 foci) (Lazaro-Pena et al., 2022).

Furthermore, as mentioned, HSF-1 is involved in various physiological and pathological processes such as differentiation, immune response, neurodegeneration, cancer and longevity (Lazaro-Pena et al., 2022). With ageing, both in mammals and *C. elegans*, proteostatic balance becomes dysfunctional leading to the formation of many age-related diseases and overall organismal metabolic stress. This is followed by reduced activation of HSF-1 resulting in proteasomal stress (Ben-Zvi et al., 2009).

HSF-1 is a transcription factor downstream of multiple signalling pathways associated with longevity - insulin-like signalling, TORC1 (TOR complex 1) signalling, dietary restriction and germline deficiency. For example, loss of germline caused by a *glp-1* mutation (abnormal Germ Line Proliferation 1, an ortholog of the NOTCH receptor) increases worm lifespan via a mechanism dependent on HSF-1 (Hansen et al., 2005). Interestingly, intermittent heat shock extends the worm's lifespan as well via HSF-1 activation.

1.2.3. Steroid Signalling

Steroid signalling is involved in many processes, from regulating developmental and reproductive timing associated with dauer menopause to the involvement in metabolism, stress, xenobiotic response and longevity (Denzel et al., 2019). Under challenging conditions, *C. elegans* larvae enter a stress-resistant dauer stage, which halts reproduction. Upon improvement of the environment, the steroid signalling pathway enables the further continuation of reproductive development by activating insulin and TGF-β(transforming growth factor beta) signalling. This results in the production of Δ4- and Δ7-dafachronic acid (DA often refers to both) by the cytochrome P450 DAF-9 (abnormal dauer formation 9) (Antebi, 2013), Rieske-like oxygenase DAF-36 (abnormal dauer formation 36) (Rottiers et al.,

2006) and others. Dafachronic acid (DA) binds to the nuclear hormone receptor DAF-12 (Motola et al., 2006), enabling DAF-12-dependent transcription of genes such as *cdr-6* (cadmium responsive 6) and *fard-1* (fatty acyl-CoA reductase 1) (Horikawa et al., 2015).

On the other hand, steroid signalling mediates longevity through different mechanisms dependent on thermosensory neurons (Lee & Kenyon, 2009). Another steroid-related lifespan-extending mechanism is induced by a loss of germline which, in addition to HSF-1, requires both DAF-16 and DAF-12 (Hsin & Kenyon, 1999). Germline loss increases the expression of *mir-81* (micro RNA 81) and *mir-241* (micro RNA 241) which inhibit AKT-1 expression and thereby activate DAF-16 (Shen et al., 2012). However, germline-less longevity depends on NHR-80, NHR-49 (Goudeau et al., 2011; Ratnappan et al., 2014) and HLH-30/TFEB (Helix Loop Helix, an ortholog of the mammalian transcription factor EB) autophagy-related genes. The latter is also required for *daf-2* and *clk-1* (clock - biological timing abnormality) lifespan extension (Lazaro-Pena et al., 2022).

1.3. NCL-1 as a Master Regulator of *Caenorhabditis elegans* Lifespan and Nucleolus Size

Previous work in the Antebi laboratory established NCL-1 (abnormal nucleoli, a TRIM2 [Tripartite Motif Containing 2] homolog) as a regulator of major longevity pathways including dietary restriction (DR) and insulin/IGF-1 signalling pathways. Although the loss of *ncl-1* did not influence wildtype lifespan, it suppressed the longevity of various long-lived mutants such as *eat-2* (EATing: abnormal pharyngeal pumping 2, a genetic model of DR), *let-363* (LEThal 363, model of reduced TOR signalling), *daf-2* (the *C. elegans* insulin/IGF receptor) and *glp-1* (germline-less mutant). It works largely downstream or parallel to protein synthesis by inhibiting FIB-1 (FIBrillarin family) and with that, maturation of rRNA (ribosomal RNA) resulting in a smaller nucleolar size (Tiku et al., 2017). This suggests that inhibition of ribosomes triggers various stress responses, which then influence lifespan extension, but the exact mechanism of *ncl-1* lifespan regulation is still not fully understood.

1.4. Co-chaperone DAF-41

To elucidate potential downstream effectors of *ncl-1,* an RNAi screen was performed to see if gene candidates could restore the lifespan of long-lived mutants in the *ncl-1* background. This entails performing lifespan experiments on either a control plate which has *E. coli* carrying information for RNA which downregulates luciferase gene (which *C. elegans* does not have) or a plate with *E. coli* which, when ingested, downregulates a gene of interest.

According to the unpublished data from the Antebi laboratory (Max Planck Institute for Biology of Ageing), the screen identified *daf-41* (Dauer Formation 41) as an interesting candidate as its downregulation was able to partially rescue the lifespan of longer-lived *glp-1* and *raga-1* (RAS-related guanosine triphosphatase-binding protein A) mutants that were suppressed by *ncl-1* mutation. Downregulation of *daf-41* in *glp-1ncl-1* mutants increased their median lifespan by 30%, and in *raga-1;ncl-1* by 7%. *Daf-41* downregulation in N2 wildtype worms, also increased their median lifespan by 11%.

DAF-41 is a *C. elegans* homolog of mammalian p23, a co-chaperone most known for modulation of HSP-90 binding affinity to client proteins. By inhibiting HSP-90 ATPase activity, it prolongs HSP-90 association with its clients (Biebl et al., 2021; Noddings et al., 2022) such as HSF-1, aryl hydrocarbon receptor or telomerase (Chen et al., 2023). Furthermore, by a similar mechanism, p23 regulates the activity of steroid hormone receptors such as progesterone receptor and glucocorticoid receptor (Knoblauch & Garabedian, 1999). After migrating to the nucleus, p23 helps in TF disassociation enabling transcription (Horikawa et al., 2015).

However, p23 is also known for its co-chaperone-independent functions, such as preventing protein aggregation (Freeman et al., 1996), acting as a tumor suppressor (Chen et al., 2023), and being one of three prostaglandin E2 synthase isoforms (PTGES3). By binding to its cognate receptors, prostaglandin E2 activates signalling pathways involved in growth control, motility, and pain perception. Additionally, PTGES limits ovarian tumor invasiveness by binding to liver-type phosphofructokinase, where it provides local PGE2 that inhibits PFKL and thereby reduces the glucose oxidation rate (Chen et al., 2023).

In *C. elegans*, DAF-41 triggers constitutive entry into dauer diapause at higher temperatures and regulates worm lifespan in a temperature-dependent manner. At 15 ºC DAF-41 prolongs wild-type lifespan through insulin/IGF-1 (DAF-16) and steroid (DAF-12) signalling and at 25 ºC shortens lifespan through DAF-16, DAF-12 and heat shock factor (HSF-1) signalling. At 20 ºC DAF-41, however, does not influence lifespan length (Horikawa et al., 2015).

2. Research Goals

The main objective of this research project is to characterize the mechanism by which DAF-41 extends the lifespan of the *glp-1ncl-1* mutant strain of *C. elegans* by investigating:

i) Whether genes from the insulin/IGF-1 signalling pathway, heat shock response genes, and steroid signalling pathway genes are involved by:

- Measuring relative expression of *daf-16 and its target genes (lipl-4, sod-3, dod-3); hsf-1 and its target genes (hsp-16.2, hsp-4, hsp-70); daf-12 and its target genes (cdr-6, fard-1), daf-36;* and *snb-1* (synaptobrevin related) as an endogenous control using the RT-qPCR method.

- Quantifying the activity of the transcription factor DAF-16 (specifically its nuclear localization) at a growing temperature to see if DAF-16 activity is changed in different mutant backgrounds. Moreover, to see if these mutations are required for DAF-16 activity in response to higher temperatures, I quantified DAF-16 activity at 37 ºC in the different mutant conditions.

- Quantifying the activity of the transcription factor HSF-1 (specifically HSF-1 foci formation) at a growing temperature to see if HSF-1 activity is changed in different mutant backgrounds. Furthermore, to determine whether these mutations are essential for HSF-1 activity at elevated temperatures, I quantified HSF-1 activity at 37 ºC in the different mutant conditions.
  - To measure DAF-16 and HSF-1 transcription factor activity, I measured the rate of their nuclear localisation and foci formation by visualizing GFP-tagged transcription factors.

ii) Whether DAF-41 regulates thermotolerance and oxidative stress resistance in *glp–1ncl–1* mutant worms by:

- Measuring heat stress resistance of N2, *glp-1, ncl-1* and *glp–1ncl–1* (both on luciferase [*luci*] and *daf-41* RNAi) as a survival percentage of worms at 37°C incubation across two hours.

- Measuring resistance of of N2, *glp-1, ncl-1* and *glp–1ncl–1* (both on *luci* and *daf-41* RNAi) to a 3-hour acute oxidative stress by exposure to 10 and 20 mmol/dm^3 hydrogen peroxide solution, and to 200 mmol/dm^3 paraquat solution.

3. Materials and methods

3.1. *Caenorhabditis elegans* Handling and Maintenance

I obtained worm strains from the Antebi Laboratory collection. I maintained the worms at 15 ºC on nematode growth media (NGM) agar Petri dishes (plates) containing a lawn of OP50 bacteria (an *Escherichia coli* strain) and transferred them onto freshly made ones every 4-10 days, depending on the strain. I maintained them either by transferring a few gravid adults onto fresh plates or by the "bleaching" method (treating them with hypochlorite, see 3.1.2 Protocol). I transferred ("picked") the worms using a platinum wire often flamed to get sterilised. Maintenance agar plates were made by laboratory technicians, while I made the plates that were part of my experiments.

The strains I used in these experiments were: N2 (wild type), *raga-1 (ok701)*, *ncl-1(e1942)*, *glp-1(e2141ts)*, *glp-1(e2141ts)ncl-1(e1942)*, *muEx265[*HSF-1*p::*HSF-1 *cDNA + myo-3::GFP]*, *daf-16(mu86)I;muIs109(Pdaf-16::daf-16::gfp;Podr-1::rfp)* and *daf-41(ok3052)* (Table 1). Additionally, I generated *daf-16::gfp;glp-1* and *daf-16::gfp;glp-1ncl-1* worms which I will describe in detail in the Materials and Methods section.

C. elegans is usually maintained and grows in 20 ºC incubators, but in these experiments, I grew all strains at 15 ºC due to the temperature sensitivity of the *glp-1* strain. *glp-1(e2141ts)* mutants' germline development is temperature sensitive. At a permissive temperature of 15 ºC, *glp-1* mutants grow normally and produce progeny, whilst at a restrictive temperature of 25 ºC, *glp-1* worms become sterile and are long-lived. To induce the *glp-1* phenotype, I grew all the strains in 25 ºC incubators from egg onwards till they reached adulthood. After reaching adulthood, I transferred the worms and further maintained at 20 ºC without the danger of *glp-1* losing its phenotype.

Table 1. C. elegans strains used in experiments alongside a short description and the role in experiments.

C. elegans STRAIN	DESCRIPTION	EXPERIMENTAL ROLE
N2	wild type	control
ncl-1(e1942)	*ncl-1* mutation that leads to loss of protein function	control
glp-1(e2141ts)III	*glp-1* mutation that leads to loss of protein function	long-lived mutant
glp-1(e2141ts)ncl-1(e1942)	double mutant	reduced lifespan (compared to *glp-1*)
muex265[hsf-1p::hsf-1 cdna + myo-3::gfp]	expresses a fused HSF-1 product with GFP (green fluorescent protein) protein	visualization of the localization of HSF-1 transcription factor
daf-16(mu86)i;muis109(pdaf-16::daf-16::gfp; podr-1::rfp)	expresses a fused DAF-16 product with GFP protein	visualization of the localization of DAF-16 transcription factor
daf-41(ok3052)	a partial deletion of *daf-41* that leads to a loss of protein function	comparison of *daf-41* deletion to *daf-41* downregulation by RNAi
raga-1(ok701)	*raga-1* mutation that leads to loss of protein function	lives longer compared to N2

3.1.1. Protocol for Preparing and Pouring the NGM Agar Plates

The following protocol gives 1 L of the NGM 2.5% agar. I mixed 3 g of NaCl, 2.5 g of peptone, 25 g of agar, 25 mL of KPO_4 (c = 1 mol/dm^3) with 1 L of ultrapure water and autoclaved for 50 min. I let it cool in 55°C water bath for 15 min. After it is cooled down, I added 1 mL of $MgSO_4$ (c = 1 mol/dm^3), 1 mL of $CaCl_2$ (c = 1 mol/dm^3), and 1 mL of cholesterol (g = 5 mg/mL in ethanol). I poured the medium into sterile Petri dishes using an automated peristaltic pump and let sit for 2-3 days to allow excess moisture to evaporate and to allow for the detection of contaminants. (Stiernagle T., 2006)

A part of maintenance agar plates was made by laboratory technicians.

3.1.2. Protocol for Treating the Worms with Hypochlorite Solution

Treatment with hypochlorite solution kills all worms but leaves the eggs intact due to their resistant shell. I used this method to synchronize the worm population or disinfect it of mould or other contaminants.

Required chemicals:

- M9 buffer

  For 1 L, dissolve 3 g of KH_2PO_4, 6 g of Na_2HPO_4, and 5 g of NaCl in 1 L of H_2O. Then, autoclave for 20 min and add 1 mL of autoclaved $MgSO_4$ (c = 1 mol/dm^3).

- Hypochlorite solution (5 mL per worm)

  I mixed 3.5 mL of M9, 0.5 mL of 5 N (normal) NaOH and 1 mL of bleach (5% solution of sodium hypochlorite).

First wash:

I washed the plate containing gravid worms with M9 buffer and transferred it into a 15 mL Falcon tube. I pelleted worms by centrifuging the tube for 1 min at 2000 rpm (rotations per minute), aspirated the supernatant and added 10 mL of M9 buffer. I repeated centrifugation and washed with M9 three more times.

Treatment with hypochlorite solution:

I gently aspirated the M9 supernatant. In the falcon tube, I added 5 mL of the hypochlorite solution, and vortexed for 7 to 9 minutes until no worms were visible. It is important not to treat the worms for more than 10 minutes because the eggs could be destroyed as well. I stopped the treatment by adding M9 buffer.

Second wash:

I centrifuged the falcon for 1 minute at 2500-3000 rpm, aspirated the supernatant and added 10 mL of M9 buffer. I shook the falcon to increase the effectiveness of the wash, as eggs tend to remain as a pellet at the bottom. I repeated the wash four more times.

Plating the worms:

The number of eggs in the solution depends on the number of initially treated gravid worms. I approximated the concentration of worms by counting the number of eggs in

10 μL and consequently putting the desired volume/number of eggs on a fresh plate with a pipette.

3.3. RNA Interference Protocol

RNA interference experiments require the preparation of special Petri dishes containing Ampicillin (Amp) and Isopropyl β-d-1-thiogalactopyranoside (IPTG). I added ampicillin as it disables the growth of any bacterial strain besides the strain I will be seeding the plates with (the strain carries Ampicillin resistance). IPTG is a commonly used inducer of gene expression of genes under the control of the lac operator. When induced, the bacterial strain seeded on these plates produces a desired double-stranded (ds) RNA which, after being eaten by worms, downregulates the corresponding genes based on RNA interference.

As a control in RNAi experiments, I used a strain carrying dsRNA which downregulates luciferase, a gene not present in *C. elegans*.

3.3.1. Protocol for Preparing and Pouring the Agar Gel in Petri dishes (plates) for RNAi

The following protocol gives 1 L of the Nematode Growth Medium (NGM) 2.5% agar. I mixed 3 g of NaCl, 2.5 g of peptone and 25 g of agar and 25 mL of KPO_4 ($c = 1$ mol/dm^3) with 1 L of ultrapure water. I autoclaved the mix for 50 min and let it cool in 55 °C water bath for 15 min. I added 1 mL of $MgSO_4$ ($c = 1$ mol/dm^3), Ampicillin* ($g = 100$ mg/mL), $CaCl_2$ ($c = 1$ mol/dm^3), IPTG ($c = 1$ mol/dm^3)* and 1 mL of cholesterol ($g = 5$ mg/mL in ethanol). I poured the medium into sterile Petri dishes using an automated peristaltic pump. I let it cool for 2-3 days to allow excess moisture to evaporate and to allow for the detection of contaminants. The protocol was adapted from Stiernagle T., 2006.

The symbol * marks chemicals specific for the RNAi plates compared to the regular NGM agar plates. I made all the RNAi plates.

3.3.2. Protocol for Inoculation and Seeding the Plates with RNAi Bacteria

Before starting, the workbench must be disinfected with a 70% ethanol solution. The protocol should be done near a source of flame. I prepared the media by adding 10 μL of Ampicillin per 10 mL of Luria-Bertani broth (LB). Before and after each step, I sterilised the top of the Erlenmeyer flask by flaming it. After adding the media in a 50 mL Erlenmeyer flask, using a pipette, I picked a small bacterial colony with a pipette tip and discarded the tip inside the flask.

I incubated Erlenmeyer flasks in a shaking incubator at 37 ºC overnight and seeded the plates with the automated pipette. On 10 cm plates, I put 450 μL of bacterial solution, and on 6 cm plates, I put 200 μL of bacterial solution. I spread the solution by gently rotating the plates. I left the plates to dry for at least two days before using them and afterward stored them in the cold room (4 °C).

3.4. Lifespan Experiments

3.4.1. Determining the Method for Lifespan Experiments

As previously mentioned, both the transfer and FUdR (5'-Fluorodeoxy Uridine) method have their advantages and disadvantages. As a first practice lifespan, I measured the lifespan of N2 and a long-lived mutant *raga-1(ok701)*, with both FUdR and transfer method. I kept and incubated the worms to develop at 20 ºC. I synchronised the worms by allowing the gravid worms to lay eggs for 3 hours after which sacrificed them, leaving their eggs on the plate to develop. At the late L4 stage (young adult), I put approximately 30 worms of each strain on two to five previously made OP50 plates.

For the transfer method, the first few days, I transferred the worms onto fresh OP50 plates every day until they stopped laying eggs. I grew the FUdR experimental group on seeded plates overlaid with FUdR (final concentration = 50 mg/mL) which were left to dry for a day before usage.

I scored the worms as dead or alive every two to four days by gently tapping them with a platinum wire. Dead worms were sacrificed by incineration. Sick worms with protruding vulva and worms that crawled to the sides of the plates were censored.

I analysed the lifespan data in Excel using the Log-Rank statistical analysis and visualised it in GraphPad Prism as a percentage of live worms on the y-axis and the number of days on the x-axis.

3.4.2. *daf-41i* lifespan experiment

I synchronised N2, *glp-1, ncl-1, glp-1ncl-1* and *daf-41* worms by hypochlorite treatment. Until L4, I grew them on *luci* RNAi and *daf-41i* plates in a 25 ºC incubator. At the late L4 stage, I transferred approximately 30 worms of each strain on previously made experimental plates. I put N2, *glp-1, ncl-1, glp-1ncl-1* on 5 *luci* plates and on 5 *daf-41* RNAi plates, while *daf-41* worms only on luciferase plates in a 20 ºC incubator. Transferring the worms to experimental plates is considered Day 1 of their adult life. For the first few days, I transferred the worms onto fresh plates until they stopped laying eggs. The worms were grown in a 20 ºC incubator from day 1 onwards.

I scored the worms as dead or alive every two to four days by gently tapping them with a platinum wire. I sacrificed dead worms by incineration and censored sick worms with protruding vulva and worms that crawled to the sides of the plates.

I analysed the lifespan data in Excel using the Log-Rank statistical analysis and visualised it in GraphPad Prism as a percentage of live worms on the y-axis and the number of days on the x-axis.

3.5. Measuring Gene Expression Using RT-qPCR

To elucidate the potential mechanism underlying observed lifespan extension caused by downregulation of *daf-41* in *glp-1ncl-1* worms, I measured gene expression of *daf-16* and its target genes (*lipl-4, sod-3, dod-3*); *hsf-1* and its target genes (*hsp-16.2, hsp-4, hsp-70*); *daf-12* and its target genes (*cdr-6, fard-1*), *daf-36*; and used *snb-1* as an endogenous control using RT-qPCR. This was done in N2, *glp-1*, *ncl-1*, and *glp-1ncl-1* grown on luciferase plates and on *daf-41* RNAi plates.

First, I prepared the 10 cm luciferase and *daf-41* plates according to the aforementioned protocol (Section 3.3). I synchronised the worms (approximately 500 worms per strain) by treatment with hypochlorite solution and then transferred the eggs onto respective *luci* and

daf-41i plates. I put worms at 25 ºC to grow for approximately 40 hours until they reached L4 stage and then I collected them in TRIzol (Invitrogen) and froze them in liquid nitrogen. I performed whole worm lysis, total RNA extraction, and cDNA (complementary deoxyribonucleic acid) synthesis using the protocols that are described below.

RT-qPCR mixture (Table 2) was distributed into 384-well plates using the JANUS pipetting robot. Each reaction had four technical replicates, including the non-template control (which did not contain RNA (cDNA), but only primers, H_2O and SYBR Master Mix).

Table 2. Single well contents of the RT-qPCR mixture.

cDNA template (1 μL template from 1 ng of RNA)	0.7 μL
primer (+) (10 μM stock)	0.5 μL
primer (-) (10 μM stock)	0.5 μL
2x **Power SYBR Green Master Mix** (ABI)	5 μL
ddH₂O	3.3 μL
total volume	10 μL

RT-qPCR was performed with The Applied Biosystems ViiA 7 system using the Power SYBR™ Green PCR Master Mix (Applied Biosystems™) in 8 biological replicates. Gene *snb*-1 served as endogenous control. I calculated the relative gene expression of all mutants using the DDC_t method and normalised their value to the N2 expression value. I statistically analysed the data using the One-way ANOVA statistical analysis and visualised it in GraphPad Prism.

3.5.1. Whole Worm Lysis and Total RNA Extraction

The following protocol is adapted from the Sigma-Aldrich kit Qiagen RNeasy/miRNeasy.

Part 1:

I washed the worms off the plate with 2 mL of M9 per 60 mm plate and spun down the worms at 2,000 rpm for 2 minutes. I washed the pelleted worms with M9 three times, until the liquid was clear, and removed as much M9 as possible. I added 750 μL of TRIzol reagent (1 mL per 10,000 worms), briefly vortexed, and transferred the solution to RNase-free EP tubes. I snap-froze the sample with liquid nitrogen and then transferred it to -80°C for long-term storage.

Part 2:

I thawed the sample in a water bath at room temperature and briefly centrifuged it at 10,000 g (rcf) for 30 seconds. In a new tube, I added 200 µL of zirconia/silica beads (for 700 µL of TRIzol). I transferred the sample to the new tube and homogenized the worms in a Qiagen Tissuelyser LT at full speed (50/s) for 15 minutes in a 4 °C room. I briefly centrifuged the sample and transferred the solution back to the original tube, discarding the beads. Approximately 600 µL of solution was recovered after homogenization. Then, I added 200 µL of chloroform per 600 µL of TRIzol and vortexed to mix. I centrifuged at no more than 12,000 g (rcf) for 15 minutes at 4 °C. I collected the top aqueous phase into a new 1.5 mL EP tube, recovering approximately 400 µL of solution, taking care not to aspirate any liquid from the layers below. I slowly added 1.5 volumes of 70-75% ethanol by pipetting and transferred the mixture to a Qiagen RNeasy Mini spin column. I centrifuged for 15 seconds at more than 8,000 g and discarded the flow-through. I added 700 µL of Buffer RW1 to the column, centrifuged for 15 seconds at more than 8,000 g, and discarded the flow-through. I prepared the DNase I incubation mix by adding 10 µL of DNase I stock solution to 70 µL of Buffer RDD, mixed by gently inverting the tube, and spun it briefly. I added the DNase I incubation mix directly to the centre of the column membrane and incubated it at room temperature for 15 minutes. I added 700 µL of Buffer RW1 to the RNeasy column, centrifuged for 15 seconds at more than 8,000 g, and discarded the flow-through. I added 500 µL of Buffer RPE, centrifuged for 15 seconds at more than 8,000 g, and discarded the flow-through. Then, I added 500 µL of Buffer RPE, centrifuged for 2 minutes at more than 8,000 g, and discarded the flow-through. I centrifuged at full speed for 1 minute to remove any residual ethanol. I transferred the column to a newly labelled 1.5 mL tube, added 50 µL of RNase-free water to the centre of the filter, waited one minute, and then centrifuged for 1 minute at full speed. I transferred the elution back onto the filter, waited one minute, and centrifuged for 1 minute at full speed. I checked the concentration and purity of the RNA on a spectrophotometer.

3.5.2. cDNA (complementary DNA) Conversion

The following is a protocol for iScript cDNA Synthesis Kit adapted from Bio-Rad. I prepared the reaction mix by adding (per reaction): 4 µL of 5x iScript Reaction Mix, 1 µL of iScript

Reverse Transcriptase, the variable volume of the RNA template (depending on the RNA concentration of the experimental condition) and the variable volume of Nuclease-free water to get the total volume of 20 μL. I incubated the reaction mix in a thermal cycler using the following protocol: priming for 5 min at 25 ºC, reverse transcription for 20 min at 46 ºC, reverse transcription (RT) inactivation for 1 min at 95 ºC and hold at 4 ºC.

I prepared the mixture of RNA template solution and water to get the cDNA concentration of 2.5 ng/μL.

3.5.3. Measuring Primer Efficiency

After obtaining primer sequences, I first checked their efficiency using different dilutions of reverse-transcribed cDNA. The total RNA was isolated and converted to cDNA using the aforementioned protocols. The cDNA concentrations used were: 5.00, 2.50, 1.25, 0.63, 0.31, and 0.16 ng/μL. The list of used primers is shown in Table 3.

Table 3. The list of primers used for measuring primer efficiency and for RT-qPCR to test the relative gene expression of snb-1, hsf-1, daf-16, daf-12 and their respective target genes (dod-3, lipl-4, sod-3; hsp-16.2, hsp-4, hsp-70; fard-1, cdr-6, daf-36) in N2, glp-1, ncl-1, glp-1ncl-1 worms with or without daf-41 downregulation and in daf-41 KO mutant.

Primer Name	Sequence (5' to 3')	From	Primer Name	Sequence (5' to 3')	From
daf-12-F	GTTCGCATCGTTACAGAACGA	Y.K. Paik, 2020, Int. K. Mol. Sci.	*dod-3*-F	CGTATATGGACCCAGCTAATG	Horikawa et al., 2015, PLoS Genet.
daf-12-R	TTCTCCTGGCAGCTCTTCG	Y.K. Paik, 2020, Int. K. Mol. Sci.	*dod-3*-R	ATGAACACCGGCTCATTC	Horikawa et al., 2015, PLoS Genet.
cdr-6-F	TCGGGCTTCTCGGTTTACC	Horikawa et al., 2015, PLoS Genet.	*fard-1*-F	TGGATCCTGAAGATGTGATGCT	Horikawa et al., 2015, PLoS Genet.

Table 3. Continuation

Primer Name	Sequence (5' to 3')	From	Primer Name	Sequence (5' to 3')	From
cdr-6-R	CAGCTTTGACCAGAGGAACCA	Horikawa et al., 2015, PLoS Genet.	*fard-1*-R	GTCGCCGCGCTATGGA	Horikawa et al., 2015, PLoS Genet.
daf-16-F	ATCAGACATCGTTTCCTTCGG	Horikawa et al., 2015, PLoS Genet.	*hsf-1*-F	GCATAACAATATGAATAGCATGGTC	Horikawa et al., 2015, PLoS Genet.
daf-16-R	TTAACCGTTTCTCTGGACTAGC	Horikawa et al., 2015, PLoS Genet.	*hsf-1*-R	GACGTCCTTGTACAAAACACGGATG	Horikawa et al., 2015, PLoS Genet.
daf-28-F	TGAACCACAAGAAGGAATTGACA	Horikawa et al., 2015, PLoS Genet.	hsp16.2-F	ACTTTACCACTATTTCCGTCCAGC	Horikawa et al., 2015, PLoS Genet.
daf-28-R	CTCGGCAGTGCATTGATAGGT	Horikawa et al., 2015, PLoS Genet.	hsp16.2-R	CCTTGAACCGCTTCTTTCTTT	Horikawa et al., 2015, PLoS Genet.
daf-36-F	GAGCAGCATGGTCCTGGAAT	Horikawa et al., 2015, PLoS Genet.	*hsp-4*-F	GTGGCAAACGCGTACTGTGATGA	Horikawa et al., 2015, PLoS Genet.
daf-36-R	ACGACTCCTTTCCCCCAAAT	Horikawa et al., 2015, PLoS Genet.	*hsp-4*-R	CGCAACGTATGATGGAGTGATTCT	Horikawa et al., 2015, PLoS Genet.
daf-41-F	GCAGCAAAACTGACAAGTACGAA	Horikawa et al., 2015, PLoS Genet.	*hsp-70*-F	AATGAACCAACTGCTGCTGCTCTT	Horikawa et al., 2015, PLoS Genet.
daf-41-R	ACGGATGCAGGATCGATTTC	Horikawa et al., 2015, PLoS Genet.	*hsp-70*-R	TGTCCTTTCCGGTCTTCCTTTTG	Horikawa et al., 2015, PLoS Genet.
sod-3-F	CACGAGGCTGTTTCGAAAGG	Horikawa et al., 2015, PLoS Genet.	*lipl-4*-F	ATGGCCGAGAAGTTCCTACATCGT	Horikawa et al., 2015, PLoS Genet.
sod-3-R	GAATTTCAGCGCTGGTTGGA	Horikawa et al., 2015, PLoS Genet.	*lipl-4*-R	GGTGAATTGGCGACCCAATCGAAA	Horikawa et al., 2015, PLoS Genet.

24

Table 3. Continuation

Primer Name	Sequence (5' to 3')	From	Primer Name	Sequence (5' to 3')	From
snb-1-F	GAATCATGAAGGTGAACGTGG	Tabrez, Antebi laboratory	***daf-12*-F**	TATCAACAAACGTGCGGCATACA	Margareta, Antebi laboratory
snb-1-R	CCAATACTTGCGCTTCAGGG	Tabrez, Antebi laboratory	***daf-12*-R**	GAAAGAACAACCTGTCCACTATC	Margareta, Antebi laboratory

When performing RT-qPCR I used four technical replicates for each sample. After performing RT-qPCR, I calculated fold change using the DDC$_t$ method. I calculated primer efficiency based on the slope value using the ThermoFisher qPCR Efficiency calculator (https://www.thermofisher.com/hr/en/home/brands/thermo-scientific/molecular-biology/molecular-biology-learning-center/molecular-biology-resource-library/thermo-scientific-web-tools/qpcr-efficiency-calculator.html).

3.6. DAF-16 Nuclear Translocation Analysis

The strains I used in this experiment were *daf-16(mu86) I; muIs109(Pdaf-16::daf-16::gfp; Podr-1::rfp)* (a strain which has a fusion protein DAF-16::GFP, I will name the strain **daf-16::gfp** hereafter for simplicity), *daf-16::gfp***;glp-1(e2141ts)** *and daf-16::gfp***;glp-1(e2141ts)ncl-1(e1942)**. Firstly, I generated *daf-16::gfp;glp-1* and *daf-16::gfp;glp-1ncl-1* worms.

3.6.1. Generation of *daf-16::gfp;glp-1* and *daf-16::gfp;glp-1ncl-1* Mutants

To elucidate how *daf-41* downregulation influences DAF-16 activity (nuclear localization of DAF-16::GFP) in *glp-1* and *glp-1ncl-1* mutants, I generated *daf-16::gfp;glp-1* and *daf-16::gfp;glp-1ncl-1* mutants. I have done this by crossing male *daf-16::gfp* worms with *glp-1* and *glp-1ncl-1* worms. The cross schematic is shown below (Figure 3).

The crosses are designed and based on the fact that *glp-1* mutants are temperature sensitive (they do not lay eggs at 25 ºC, but do at 15 ºC) and the fact that under a fluorescent microscope, one can observe whether a population of worms is homozygous or heterozygous for DAF-16::GFP.

$$P0: \; \male \; \frac{GFP}{GFP} \frac{+}{+} \; x \; \frac{+}{+} \frac{glp-1}{glp-1} \; \hermaphrodite$$

$$F1: \; \hermaphrodite \male \; \frac{GFP}{+} \frac{glp-1}{+}, \; \frac{+}{+} \frac{glp-1}{glp-1} \; \hermaphrodite$$

$$F2: \; \hermaphrodite \; \frac{GFP}{GFP} \frac{+}{+}, \; \frac{GFP}{GFP} \frac{glp-1}{+} \; \male, \; \frac{GFP}{GFP} \frac{glp-1}{glp-1} \; \male, \; \frac{GFP}{+} \frac{+}{+} \; \male, \; \frac{GFP}{+} \frac{glp-1}{+} \; \male, \; \frac{GFP}{+} \frac{glp-1}{glp-1} \; \male,$$

$$\frac{+}{+} \frac{+}{+} \; \male, \; \frac{+}{+} \frac{glp-1}{+} \; \male, \; \frac{+}{+} \frac{glp-1}{glp-1} \; \hermaphrodite$$

$$F3: \; \hermaphrodite \; \frac{GFP}{GFP} \frac{+}{+}, \; \frac{GFP}{GFP} \frac{glp-1}{+} \; \male, \; \frac{GFP}{GFP} \frac{glp-1}{glp-1} \; \male, \; \frac{GFP}{+} \frac{+}{+} \; \male, \; \frac{GFP}{+} \frac{glp-1}{+} \; \male, \; \frac{GFP}{+} \frac{glp-1}{glp-1} \; \hermaphrodite,$$

$$\frac{+}{+} \frac{+}{+} \; \male, \; \frac{+}{+} \frac{glp-1}{+} \; \male, \; \frac{+}{+} \frac{glp-1}{glp-1} \; \hermaphrodite$$

$$P0: \; \male \; \frac{GFP}{GFP} \frac{+}{+} \frac{+}{+} \; x \; \frac{+}{+} \frac{glp-1}{glp-1} \frac{ncl-1}{ncl-1} \; \hermaphrodite$$

$$F1: \; \hermaphrodite \male \; \frac{GFP}{+} \frac{glp-1}{+} \frac{ncl-1}{+}, \; \frac{+}{+} \frac{glp-1}{glp-1} \frac{ncl-1}{ncl-1} \; \hermaphrodite$$

$$F2: \; \hermaphrodite \; \frac{GFP}{GFP} \frac{+}{+} \frac{+}{+}, \; \frac{GFP}{GFP} \frac{glp-1}{+} \frac{ncl-1}{+} \; \male, \; \frac{GFP}{GFP} \frac{glp-1}{glp-1} \frac{ncl-1}{ncl-1} \; \male,$$

$$\frac{GFP}{+} \frac{+}{+} \frac{+}{+} \; \male, \; \frac{GFP}{+} \frac{glp-1}{+} \frac{ncl-1}{+} \; \male, \; \frac{GFP}{+} \frac{glp-1}{glp-1} \frac{ncl-1}{ncl-1} \; \male,$$

$$\frac{+}{+} \frac{+}{+} \frac{+}{+} \; \male, \; \frac{+}{+} \frac{glp-1}{+} \frac{ncl-1}{+} \; \male, \; \frac{+}{+} \frac{glp-1}{glp-1} \frac{ncl-1}{ncl-1} \; \hermaphrodite$$

$$F3: \; \hermaphrodite \; \frac{GFP}{GFP} \frac{+}{+} \frac{+}{+}, \; \frac{GFP}{GFP} \frac{glp-1}{+} \frac{ncl-1}{+} \; \male, \; \frac{GFP}{GFP} \frac{glp-1}{glp-1} \frac{ncl-1}{ncl-1} \; \male,$$

$$\frac{GFP}{+} \frac{+}{+} \frac{+}{+} \; \male, \; \frac{GFP}{+} \frac{glp-1}{+} \frac{ncl-1}{+} \; \male, \; \frac{GFP}{+} \frac{glp-1}{glp-1} \frac{ncl-1}{ncl-1} \; \male,$$

$$\frac{+}{+} \frac{+}{+} \frac{+}{+} \; \male, \; \frac{+}{+} \frac{glp-1}{+} \frac{ncl-1}{+} \; \male, \; \frac{+}{+} \frac{glp-1}{glp-1} \frac{ncl-1}{ncl-1} \; \hermaphrodite$$

Figure 3. Schematic of crossing daf-16::gfp with glp-1 and glp-1ncl-1 strains. Glp-1 and ncl-1 are located on the same chromosome and are often inherited together. Paternal strains (P0) are daf-16::gfp –> homozygous for a DAF-16::GFP fusion gene and wildtype glp-1 phenotype (depicted as +) and glp-1 or glp-1ncl-1 – > homozygous mutant for a deletion of glp-1 or glp-1ncl-1 genes and with a wildtype genotype for the daf-16::gfp (depicted as +). Parent daf-16::gfp was male and glp-1 or glp-1ncl-1 mutant were hermaphrodite. Their progeny F1 (Filial 1) is heterozygous for daf-16::gfp and glp-1 (or glp-1ncl-1) mutation and will be both male and hermaphrodite (depicted in orange color). A part of F1 generation will be hermaphrodite glp-1 mutants that are a product of selfing (self-fertilisation) of hermaphrodite P0 glp-1 mutants. Because I selected heterozygous hermaphrodite from F1, only their F2 progeny (from selfing) is shown in the schematic. In the second selection process, I am screening for the daf-16::gfp;glp-1 or daf-16::gfp;glp-1ncl-1 homozygous mutants (depicted purple).

To generate male *daf-16::gfp* worms, I have put a few L4 *daf-16::gfp* worms in the 32 ºC incubator for 5 hours. Part of the progeny of these worms ends up being male due to the heat stress.

I put 8-10 male *daf-16::gfp* worms (♂ GFP/GFP +/+) on a small 3 cm OP50 plate with 4-6 hermaphrodite *glp-1* mutants (+/+ *glp-1/glp-1* ⚥).

The next day and the day after that, I transferred the parental generation to fresh 3 cm plates. The day after that, I transferred the parents onto a fresh 6 cm OP50 plate. When their progeny (F1 generation) developed to the L3 or L4 stage, I picked 10 individual F1 worms into 10 individual OP50 plates. After they developed into gravid worms and laid eggs for one day, I transferred these F1 worms onto fresh 10 replicate plates and put the plates with F2 eggs in the 25 ºC incubator. I put the fresh replicate plates with F1 worms at 15 ºC to lay eggs for one day as well. After sacrificing the F1 worms, I grew the F2 eggs at 15 ºC into F2 adults. After the F2 adults at 25 ºC had developed, I checked if they laid eggs. Homozygous F2 worms (+/+ *glp-1/glp-1* ⚥) are a result of hermaphrodite selfing of F1 (+/+ *glp-1/glp-1* ⚥) worms and will not lay progeny at 25 ºC. As I was interested in the progeny of F1 heterozygous hermaphrodites (GFP/+ *glp-1/+* ⚥, orange in the Figure 3 schematic), I took note of the plates where F2 worms did lay eggs as it meant they were heterozygous for both *glp-1* and *daf-16::gfp*.

At that point, I returned to the corresponding replicate plates that were kept at 15 ºC and singled out the F2 worms with a heterozygous F1 parent onto 20 plates. This time I had to single out more worms as the probability of picking a homozygous worm is much lower. After they laid eggs for a day, I transferred these F2 worms onto fresh 20 replicate plates, while the plates with F3 eggs were put in the 25 ºC incubator. I put the fresh plates with F2 worms at 15 ºC to lay eggs for one day as well. The F2 worms were sacrificed, while the eggs were left to develop at 15 ºC into F3 adults. After the F3 adults at 25 ºC had developed, I checked if they laid eggs. Homozygous F3 worms (GFP/GFP *glp-1/glp-1* ⚥, purple in the Figure 3 schematic) are a result of hermaphrodite selfing of the desired F2 (GFP/GFP *glp-1/glp-1* ⚥, purple in the Figure 3 schematic) worms and will not lay progeny at 25 ºC. As I was interested in these worms, I took note of the plates that had these F2 parents. To check if corresponding F3 worms at 15 ºC were homozygous for the *daf-16::gfp* gene as well, I exposed the worms to heat stress by putting them in the 37 ºC incubator for 1.5 hours to induce DAF-16::GFP nuclear translocation. Then,

I checked under a microscope if all the F3 progeny had the nuclear signal or not. If they had, it meant they were probably homozygous for *daf-16::gfp*.

The same protocol was done with *glp-1ncl-1* mutants except at the end we validated the *ncl-1* mutation by looking at the nucleolar size of 20 individual F3 worms.

To confirm the generation of *daf-16::gfp;glp-1* and *daf-16::gfp;glp-1ncl-1* mutants, I genotyped the candidates for GFP using the aforementioned protocol.

3.6.2. Genotyping

I singled out multiple candidates and waited a day for them to lay eggs. Then, I lysed the worms using the Single Worm Lysis protocol and checked their genotype with a PCR reaction and gel electrophoresis. For the controls, I genotyped wild-type N2 worms and *daf-16::gfp* mutants.

Single Worm Lysis Protocol

Single Worm Lysis Buffer is made by mixing 50 mM KCl, 10 mM Tris-HCl (pH 8.3), 2.5 mM MgCl$_2$, 0.45% Nonidet P-40, 0.45% Tween 20 and 0.01% (w/v) gelatine. It is autoclaved and stored as aliquots at −20 °C. It was made by laboratory technician and stored in the media kitchen.

For 10 samples of the Lysis Mix, I added 95 μL of Single worm lysis buffer in a 1.5 mL Eppendorf tube. To this, I added 5 μL of Proteinase K (stored at – 20 °C in the common freezer), and shortly vortexed the mix and spun it down.

I labelled the PCR plate, the wells, and the worm plates from which the worms were collected. I put 10 μL of the Lysis Mix in each well of the PCR plate and picked 1 worm from the labelled worm plate into the designated well. I closed wells with caps and made sure to double-check if it is closed. I put the PCR plate for 30 min into a -80 °C freezer. After this, I put the plate into the PCR machine and started the lysis program: 1. 65 °C 60 min, 2. 95 °C 15 min, 3. 4 °C endless.

PCR Protocol

I prepared the master mix without the lysate (Table 4). Per reaction, I added:

Table 4. Master mix preparation details for worm genotyping.

	DreamTaq DNA Polymerase (5 U/µL)	Primer 1	Primer 2	(Optional Primer 3)	Single Worm Lysate	Ultrapure water	Total
Volume per reaction	10 µL	1 µL	1 µL	(1 µL)	3-4 µL	To the total volume	20 µL

In addition to the prepared lysates, I prepared an "artificial heterozygote" by mixing 2 µL of wildtype and 2 µL of the mutant lysate.

The PCR run details for detecting the GFP *gene* were 95 °C 3 min, 95 °C 30 sec, 59 °C 30 sec (repeat 35x), 72°C 1 min, 72°C 5 min, 4 °C.

Gel Electrophoresis

I prepared 50 mL of 2% agarose gel by mixing 1 g of agarose with 50 mL of 1x TAE (Tris-acetate-EDTA) buffer. I microwaved for two to three minutes, while gently swirling a few times until the agarose was dissolved. After the gel had cooled a little, I added 2.5 µL of ROTI®GelStain (a less-toxic alternative for fluorescent staining of nucleic acids compared to ethidium bromide). After assembling the gel casting tray and the comb, I poured the gel and waited for 30 min for it to polymerise. After this, I put the gel in the horizontal electrophoretic gel tank and carefully removed the comb. I ran the gel at 120 V for 15 to 20 min and imaged it with the Bio-Rad ethidium bromide gel imaging system.

3.6.3. DAF-16 Activity Analysis

daf-16::gfp, daf-16::gfp;glp-1 and *daf-16::gfp;glp-1ncl-1* were grown on luciferase and *daf-41* RNAi plates. As a control, I grew *daf-16::gfp* on *daf-16* RNAi and *daf-2* RNAi [it is known that *daf-2* mutants accumulate DAF-16 in the nucleus in many cell types (Libina et al., 2003)]. I have put approximately 20 gravid worms of each strain to lay eggs at 15 ºC for 1.5 hours. After sacrificing adults, I left the eggs to develop at 25 ºC into the L4 stage.

I imaged hypodermal cells in the tail region with a Zeiss Axio Imager Z1 Fluo- Microscope. I immobilized approximately 10 worms of each condition on 2% agarose (previously put on glass slides) using 2 mL of sodium azide solution (NaN$_3$, c=10mM). After putting immersive oil on the slide cover, I took the pictures using both DIC and GFP fluorescent channels with a 100x objective and an exposure time of 500 ns.

Under the condition of heat stress, it is known that DAF-16 is nuclear localised. I wanted to investigate if NCL-1 and subsequently *daf-41* downregulation play a role in regulating DAF-16 nuclear localisation upon heat stress or not. To measure this, I imaged all the different strains (L4) at 37 ºC for 1.5 hours. I took the images with a 100x objective and an exposure time of 1500 ns.

Based on the intensity of DAF-16 nuclear foci, I classified the worms as having no nuclear signal (DAF-16::GFP is located in the cytoplasm), medium (DAF-16::GFP is located both in cytoplasm and nucleus) or strong signal (DAF-16::GFP is located in the nucleus). I calculated the ratio of the number of worms in each group compared to the total number of worms in the biological replicate.

I did the experiments in 1-4 biological replicates. I visualized and analysed the data in GraphPad Prism using the Standard one-way ANOVA statistical analysis.

3.7. HSF-1 Activity Analysis

The strain I used in this experiment was *muEx265[*HSF-1*p::HSF-1 cDNA + myo-3::GFP]* (a strain which has a fusion protein HSF-1::GFP, shorter *hsf-1::gfp*). I grew *hsf-1::gfp* on luciferase and *daf-41* RNAi plates. As a control, I grew *hsf-1::gfp* on *hsf-1* RNAi. I left approximately 20 gravid worms of each strain to lay eggs at 15 ºC for 1.5 hours. After sacrificing adults, I left the eggs to develop at 25 ºC into the L4 stage.

I imaged hypodermal cells in the tail region with a Zeiss Axio Imager Z1 Fluo-Microscope. I immobilized approximately 10 worms of each condition on 2% agarose (previously put on glass slides) using 2 mL of sodium azide solution (NaN$_3$, c=10mM). After putting immersion oil on the slide cover, I took the pictures using both DIC and GFP fluorescent channels with a 100x objective lens and an exposure time of 500 ns. To measure HSF-1 activity at 20 ºC, I

calculated the number of GFP nuclei compared to the total number of hypodermal tail nuclei per worm.

To measure if higher temperature influenced HSF-1 nuclear activity in different mutant backgrounds, I put all conditions at the L4 stage at 37 ºC for 30 min and took images with a 100x objective and an exposure time of 500 ns, using both the DIC and GFP fluorescent channels. To measure HSF-1 activity at 37 ºC, I calculated the number of GFP nuclei compared to the total number of hypodermal tail nuclei per worm.

I did the experiments in two biological replicates. I visualised and analysed the data in GraphPad Prism using the Standard one-way ANOVA statistical analysis.

3.8. Heat Stress Resistance Assay

To synchronise the strains, I put twenty gravid adult N2, *glp-1*, *ncl-1*, *glp-1ncl-1* and *daf-41* worms on pre-made luciferase and *daf-41* RNAi plates to lay eggs in 15 ºC incubators. After 1.5 hours, the adults were sacrificed and the eggs were put in 25 ºC incubators to develop to the L4 stage. Then, I put the worms into the 37 ºC incubator (heat stress) for 1:00, 1:15, 1:30, 1:45 and 2:00 hours. After stopping the heat stress, I transferred the worms to 20 ºC incubators to recover. After 13 to 14 hours, I scored and calculated the survival percentage.

Each condition had approximately 200 worms per biological replicate, and there were at least four biological replicates overall.

I analysed and visualised the data in GraphPad Prism. The data was statistically analysed using Ordinary two-way ANOVA analysis.

3.9. Oxidative Stress Resistance Assay

Similarly to the heat stress resistance assay, to synchronize the strains, I put twenty gravid adult N2, *glp-1*, *ncl-1*, *glp-1ncl-1* and *daf-41* worms on pre-made luciferase and *daf-41* RNAi plates to lay eggs in 15 ºC incubators. As *clk-1* worms have decreased survival compared to wild-type, and as *isp-1* worms have increased survival compared to wild-type (Senchuk et al., 2017), I used these strains as positive controls. After 1.5 hours, I sacrificed the adults, and put the eggs in 25 ºC incubators to develop to the L4 stage. Then I transferred the worms to well-plates containing 10 mmol/dm^3 H$_2$O$_2$, 20 mmol/dm^3 H$_2$O$_2$ or 100 mmol/dm^3 paraquat solution (I

previously prepared in M9 buffer). I put approximately 30 worms of each condition in a well with two to three technical replicates per biological replicate. I scored the worms for survival after 1, 2 and 3 hours for the 20 mmol/dm^3 H$_2$O$_2$ treatment, and after 3 hours of 10 mmol/dm^3 H$_2$O$_2$ and paraquat treatment. The experiment testing the 10 mM H$_2$O$_2$, and 100 mM paraquat resistance were done in three biological replicates, whilst the 20 mM H$_2$O$_2$ resistance experiment had one biological replicate.

I analysed and visualised the data in GraphPad Prism. I statistically analysed the 10 mM H$_2$O$_2$, and 100 mM paraquat experiments using Ordinary one-way ANOVA analysis, whilst the 20 mM H$_2$O$_2$ experiment using Ordinary two-way ANOVA analysis. One-way ANOVA analysis was used because I compared strains at one time point for the 10 mM H$_2$O$_2$, and 100 mM paraquat experiments whilst for the 20 mM H$_2$O$_2$ experiment I used two-way ANOVA as I compared strains at multiple time points.

4. Results

4.1. Lifespan Experiments

4.1.1. Determining the Method for the Lifespan Experiments

To test if the transfer or FUdR method is more suitable for lifespan experiments throughout my project, I compared the mean, maximum and median lifespan of N2 and *raga-1* worms using these two different methods.

N2 and *raga-1* mutant worms lived significantly longer and had the higher mean, median and maximum lifespan when the experiment was done with the transfer method compared to the FUdR method (Table 5, Figure 4).

There was no significant difference between the mean lifespan of N2 and *raga-1* worms in both cases (FUdR method -> *raga-1* (19.3 days) - N2 (17.9 days) = 1.4 days, transfer method -> *raga-1* (24.5) - N2 (20.8) = 3.7 days).
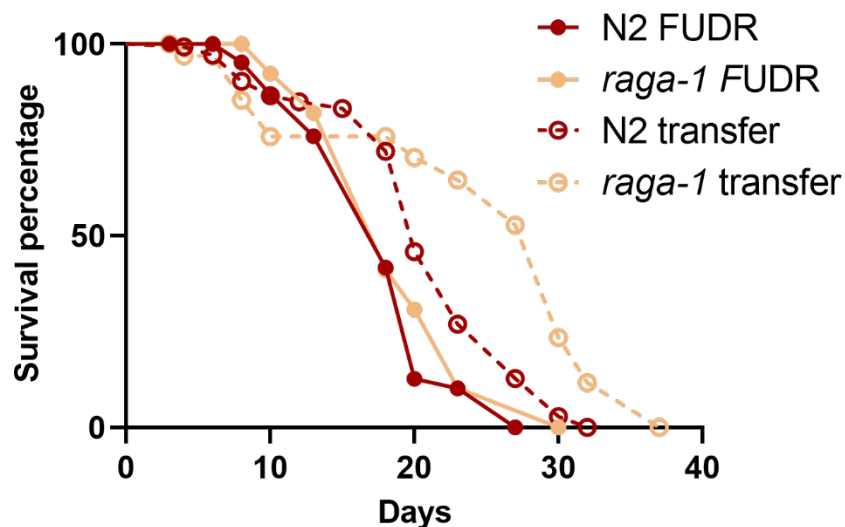

Figure 4. N2 and raga-1 lifespan depicted as a survival percentage across days. N2 and raga-1 lifespans were done with FUdR and transfer method. Both N2 and raga-1 lived significantly longer and had a higher median lifespan if transferred compared to the treatment with FUdR. Raga-1 worms lived longer than N2 when using either method, but the difference was higher in non-treated groups (transfer). N (number of worms per biological replicate) = 20-160, n (biological replicate) = 1. The data was analysed using the Log-Rank statistical analysis.

The P-values are presented in Table 6. Although it was insignificant, the difference between the mean, median and maximum lifespan of N2 and raga-1 worms was higher when using the transfer method than the FUdR. For this reason, I used the transfer method when measuring the influence of *daf-41* downregulation on worm lifespan.

Table 5. N2 and raga-1 lifespan experiment details. Here are shown the mean, median and maximum lifespan, number of total worms, censored worms and worms that died per experimental group. The mean and maximum lifespan of N2 and raga-1 was much higher when measured using the transfer method compared to the FUdR method.

	N2 FUdR	raga-1 FUdR	N2 transfer	raga-1 transfer
Mean Lifespan	17.93	19.33	20.84	24.51
Median Lifespan	18	18	20	30
Maximum Lifespan	27	30	32	37
Number of Total Worms	160	20	150	36
Number of Died Worms	94	10	86	18
Number of Censored Worms	66	10	64	18

Table 6. P-values of log-rank test on median lifespan values of N2 and raga-1 worms using the transfer (t) or FUdR method. There is no significant difference between the median lifespan length between N2 and raga-1 when using both methods (p>0.05). While the difference in raga-1 median lifespan between the methods is larger it is statistically insignificant. The difference in N2 median lifespan length between the methods is significant.

N2 FUdR vs	N2 t vs	*raga-1* FUdR vs	N2 FUdR vs
***raga-1* FUdR** p = 0.41	*raga-1* t p = 0.14	*raga-1* t p = 0.051	N2 t p = 1.33 x 10^{-13}

4.1.2. *daf-41* Downregulation Influences *Caenorhabditis elegans* Lifespan

To see how *daf-41* downregulation influences *glp-1ncl-1* lifespan, and to gain more insight in *daf-41* influence on worm lifespan, I performed lifespan experiments in N2, *glp-1*, *ncl-1*,

glp-1ncl-1 and *daf-41* mutants, both on *luci* and *daf-41i* RNAi plates (Figure 5). Their mean, median and maximum lifespans, along with the number of total experimental worms, the number of worms that died and that were censored due to protruded vulva or migrating out of the plate are shown in Table 7. The comparison p-values using the Log-rank analysis are shown in Table 8.

Table 7. Lifespan experiment details of N2, ncl-1, glp-1, glp-1ncl-1, N2 daf-41i, ncl-1 daf-41i, glp-1ncl-1 daf-41i and daf-41 worms. Here are shown the mean, median and maximum lifespan in days, number of total worms, censored worms and worms that died per experimental group.

	N2	ncl-1	glp-1	N2 daf-41i	ncl-1 daf-41i	glp-1 daf-41	glp-1ncl-1	glp-1ncl-1 daf-41i	daf-41
Mean Lifespan	19.8	17.88	40.62	14.73	16.82	41.35	26.44	31.16	14.37
Median Lifespan	20	18	43	14	18	39	28	31	14
Maximum Lifespan	32	25	64	27	25	64	43	49	28
Number of **Total** Worms	156	166	150	151	152	150	162	127	90
Number of **Died** Worms	110	84	140	121	97	118	119	79	56
Number of **Censored** Worms	46	82	10	30	55	32	43	48	34

glp-1 worms lived significantly longer than N2 (115% higher median lifespan) (Figure 5-C), while *ncl-1* mutants had a significantly shorter median (by 10%) and maximum lifespan than N2 (by 22%) (Figure 5-B). *Daf-41* downregulation did not significantly influence the lifespan of *glp-1* and *ncl-1* worms (Figures 5-B, C), but *daf-41* downregulation in *glp-1ncl-1* worms partially rescued *glp-1* longevity and increased *glp-1ncl-1* median lifespan by 11% (31/28 days) (Figure 5-D).

On the other hand, *daf-41* downregulation in wildtype condition (N2) decreased median lifespan by 30% (14/20). *daf-41* knock-out mutant also had a decreased median and maximum lifespan compared to N2, and to the same extent as worms with *daf-41* downregulation (by 30%, 14/20) (Figure 5-A).
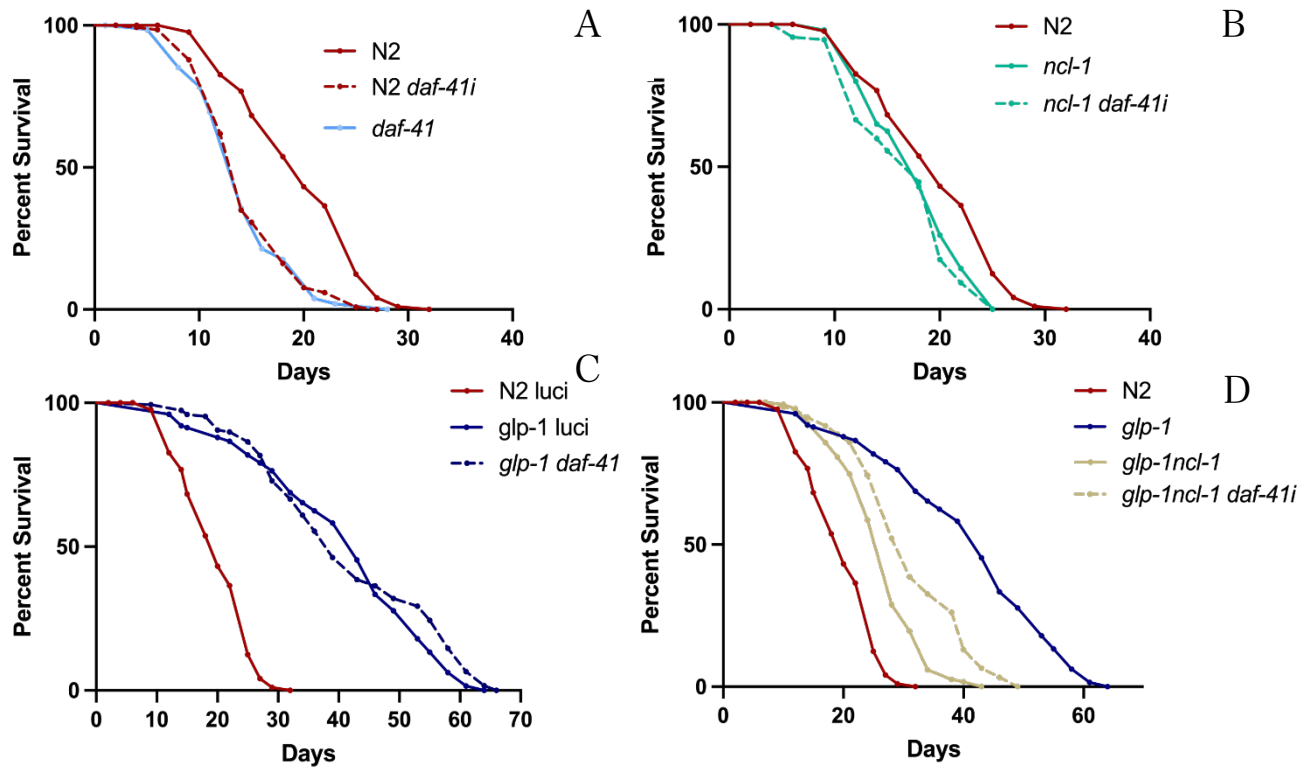

Figure 5. Lifespan of N2, glp-1, ncl-1, glp-1ncl-1, N2 daf-41i, ncl-1 daf-41i, glp-1ncl-1 daf-41i and daf-41 worms. (A) daf-41 downregulation in wildtype N2 decreased median lifespan by 30%. The daf-41 knockout mutant also had a 30% decrease in median and maximum lifespan compared to N2. (B)(C) daf-41 downregulation did not significantly affect the lifespan of glp-1 and ncl-1 worms. (B) ncl-1 mutants had a 10% shorter median and 22% shorter maximum lifespan compared to N2. (C) glp-1 worms lived significantly longer than N2. (D) daf-41 downregulation in glp-1ncl-1 worms partially rescued glp-1 longevity, increasing their median lifespan by 11%. The data was analysed using the Log-rank statistical test. N = 90-166 n=1

Table 8. P-values of the lifespan length differences between N2, ncl-1, glp-1, glp-1ncl-1, N2 daf-41i, ncl-1 daf-41i, glp-1ncl-1 daf-41i and daf-41 worms. The test used was the Log-rank statistical analysis.

N2 versus		ncl-1 versus		glp-1 versus		glp-1ncl-1 versus	
ncl-1	$p = 9.3 \times 10^{-4}$	ncl-1 daf-41i	$p = 0.23$	glp-1 daf-41i	$p = 0.89$	glp-1ncl-1 daf-41i	$p = 5.1 \times 10^{-4}$
glp-1	$p = 4.3 \times 10^{-39}$	glp-1ncl-1	$p = 4.9 \times 10^{-16}$	glp-1ncl-1	$p = 5.7 \times 10^{-34}$		
N2 daf-41i	$p = 2.3 \times 10^{-13}$						
daf-41	$p = 3.4 \times 10^{-11}$						

4.2. Measuring Gene Expression Using RT-qPCR

To determine if the regulation of lifespan by the DAF-41 protein is mediated through the insulin signaling pathway, steroid signaling pathway, or heat shock response signaling pathway, I measured the expression of their characteristic genes (insulin: *daf-16, lipl-4, sod-3, dod-3*; heat shock: *hsf-1, hsp-16.2, hsp-4, hsp-70*; steroid: *daf-12, daf-36, cdr-6, fard-1;* and *snb-1* as an endogenous control) using the RT-qPCR method in N2, *glp-1*, *ncl-1* and *glp-1ncl-1* mutants, both on *luci* and *daf-41i* RNAi plates.

4.2.1. Primer Efficiency

Primer efficiency was calculated and is shown based on data shown in Table 9 and Figure 6.
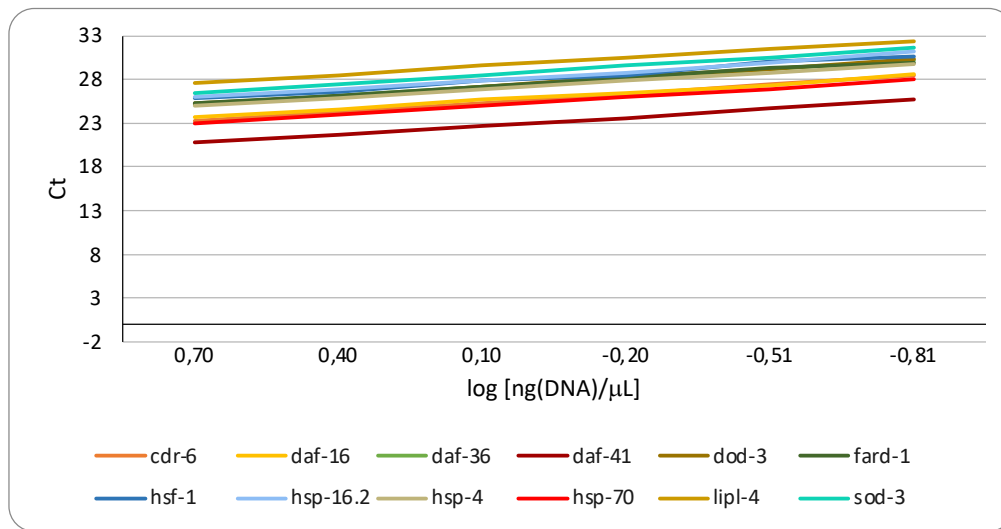

Figure 6. Primer qPCR efficiency. The figure shows average Ct values of primers cdr-6, daf-12, daf-16, daf-36, daf-41, dod-3, fard-1, hsf-1, hsp-16.2, hsp-4, hsp-70, lipl-4 and sod-3 for different raga-1 DNA concentrations: 0.15, 0.31, 0.63, 1.25, 2.5 and 5.0 ng/mL.

Table 9. RT-qPCR primer efficiency data. It shows average C_t (cycle thershold) values for different DNA concentrations (0.15, 0.31, 0.63, 1.25, 2.5, 5.0 ng/mL) for primers cdr-6, daf-12, daf-16, daf-36, daf-41, dod-3, fard-1, hsf-1, hsp-16.2, hsp-4, hsp-70, lipl-4 and sod-3. For each data subset, the efficiency was calculated based on the slope value using the ThermoFisher qPCR Efficiency Calculator.

ng(DNA)µL	cdr-6	daf-16	daf-36	daf-41	dod-3	fard-1	hsf-1	hsp-16.2	hsp-4	hsp-70	lipl-4	sod-3
5	23.3	23.65	25.19	20.79	25.31	25.25	25.86	26.04	24.93	22.99	27.6	26.49
2.5	24.26	24.63	26.15	21.63	26.05	26.16	26.55	26.9	25.83	23.92	28.5	27.45
1.25	25.3	25.76	27.09	22.69	27.22	27.15	27.86	27.95	26.82	24.95	29.57	28.42
0.63	26.28	26.48	28.09	23.61	28.34	28.1	28.51	28.81	27.82	25.93	30.47	29.57
0.31	27.41	27.33	29.17	24.77	29.15	29.27	30.02	29.87	28.79	26.88	31.54	30.51
0.16	28.42	28.66	30.19	25.71	30.39	29.96	30.58	31.25	29.77	28.09	32.4	31.58
slope	-3.42	-3.21	-3.32	-3.32	-3.4	-3.21	-3.29	-3.4	-3.24	-3.36	-3.23	-3.4
efficiency	96.18%	104.71%	99.88%	100.20%	96.83%	104.98%	101.33%	96.77%	103.65%	98.45%	104.16%	96.97%

All primers except *daf-12* had a high efficiency of gene amplification. The *daf-12* primers did not amplify at all.

4.2.2. Changes in Gene Expression Following *daf-41* Downregulation

Figures 7, 8 and 9 show relative gene expression of *daf-16* and its target genes (*lipl-4, sod-3, dod-3*); *hsf-1* and its target genes (*hsp-16.2, hsp-4, hsp-70*); *daf-12* and its target genes (*cdr-6, fard-1*) and *daf-36* in N2, *glp-1*, *ncl-1*, *glp-1ncl-1* worms with or without *daf-41* downregulation. *snb-1* was used as an endogenous control, and expression levels of all strains were normalised to N2 grown on luciferase.

Daf-41 downregulation did not significantly influence the expression of most genes in any genetic background. Moreover, there is no significant difference in gene expression when comparing *glp-1*, *glp-1ncl-1* and *glp-1ncl-1 daf-41i* mutants.

However, there were certain trends and significant differences in gene expression amongst different mutants. To simplify, I will only mention statistical significance if the difference was significant.

Expression of **hsf-1** (Figure 7) was slightly upregulated in *glp-1* worms. Moreover, knocking down *daf-41* in either N2 or *glp-1* showed a slight upregulation. Interestingly, *ncl-1* mutation in both wildtype background and *glp-1* background significantly reduced *hsf-1* expression, although downregulating *daf-41* had no significant effects. A similar trend can be observed for the expression of the *hsf-1* target gene **hsp-4**. However, **hsp-16.2** expression levels were slightly lower in *glp-1* and *ncl-1* worms compared to wildtype, and conversely, *daf-41* downregulation increased expression levels compared to N2. Furthermore, double *glp-1ncl-1* mutants had a higher level of *hsp-16.2* expression compared to single mutants, and *daf-41* downregulation further increased its expression level.

A similar trend can be observed for the expression of **hsp-70**, but the *daf-41* downregulation increased gene expression to a further extent in *N2* and *glp-1* mutants, but not in *ncl-1* mutants alone.
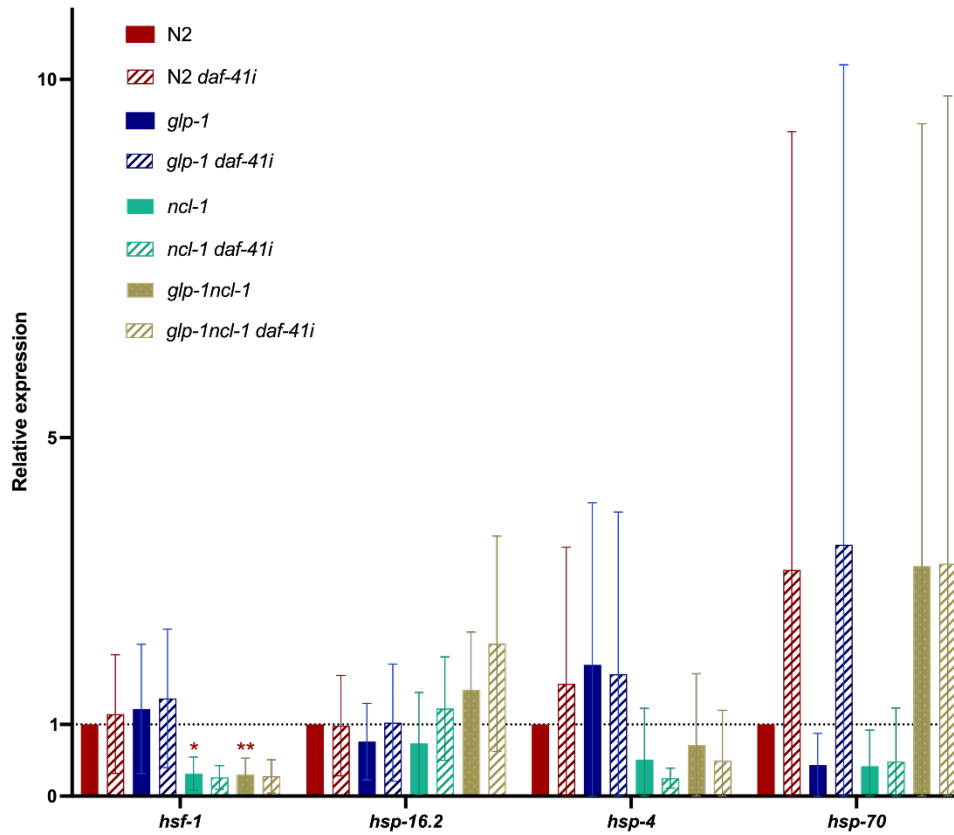
hsf-1 and *hsf-1* target gene expression

*Figure 7. Relative gene expression of hsf-1and respective target genes hsp-16.2, hsp-4, hsp-70 in N2, glp-1, ncl-1, glp-1ncl-1 worms with or without daf-41 downregulation. Experimental strains that had daf-41 downregulated are depicted with striped patterns. Number of worms per condition N= 500, biological replicates n=8, four technical replicates. The data was statistically analysed using Ordinary one-way ANOVA analysis. *p<0.05, **p<0.01 compared to N2. Error bars show SEM (standard error) based on fold changes across 8 biological replicates.*

The expression of **daf-16** (Figure 8) is upregulated in all conditions.

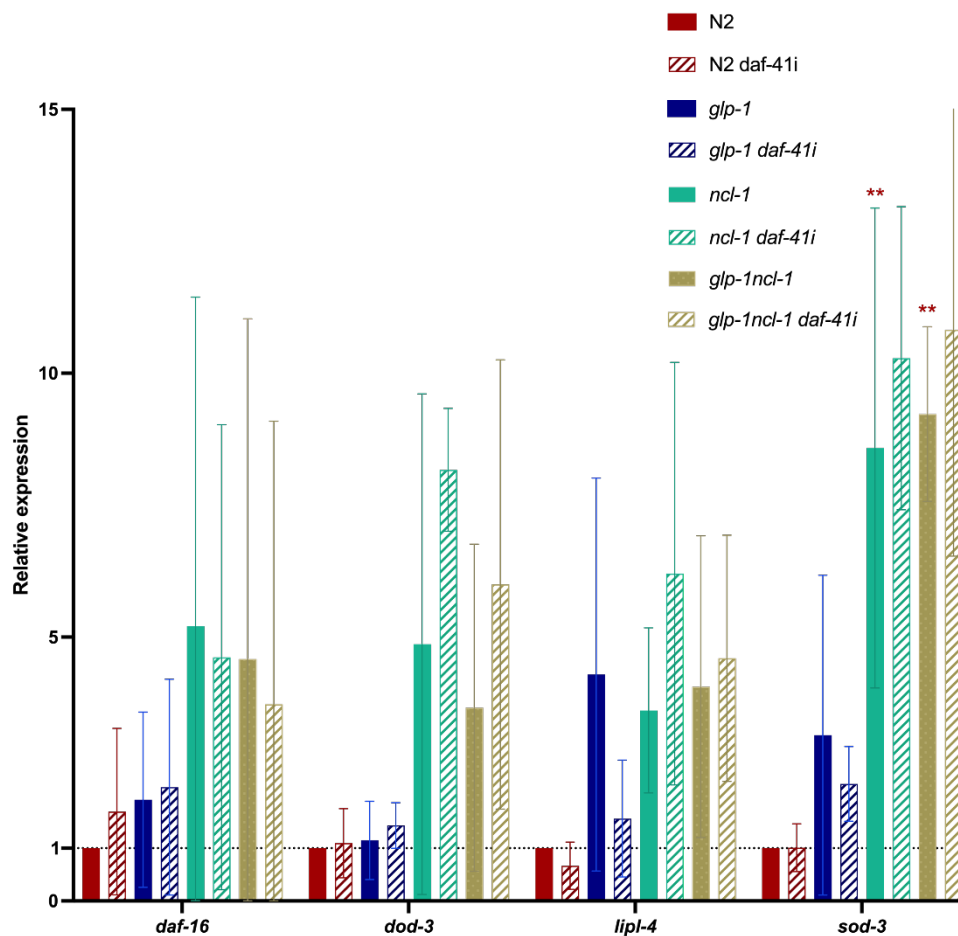## *daf-16* and *daf-16* target gene expression

Figure 8. Relative gene expression of daf-16 and respective target genes (dod-3, lipl-4, sod-3) in N2, glp-1, ncl-1, glp-1ncl-1 worms with or without daf-41 downregulation. Experimental strains that had daf-41 downregulated are depicted with striped patterns. Number of worms per condition N= 500, biological replicates n=8, four technical replicates. The data was statistically analysed using Ordinary one-way ANOVA analysis. **p<0.01 compared to N2. Error bars show SEM (standard error) based on fold changes across 8 biological replicates.

There was a trend where the loss of *ncl-1* upregulated expression of *daf-16* target genes **sod-3** and **dod-3**. Both genes were upregulated in *ncl-1* compared to N2 (significant for *sod-3*) and in *glp-1ncl-1* compared to *glp-1* worms. A similar trend was observed for **lipl-4** expression, however, loss of *ncl-1* did not upregulate *lipl-4* expression in *glp-1ncl-1* mutants compared to *glp-1* (which already had upregulated *lipl-4* compared to N2).

Downregulation of *daf-41* did not significantly influence *daf-16* and *daf-16* target gene expression, but it did tend to upregulate most genes in *ncl-1* background (in *ncl-1* and *glp-1ncl-1* mutants). Interestingly, *daf-41* downregulation did not influence gene expression in wildtype background (N2 *daf-41i*).

The expression of *daf-12*-related genes in *glp-1* was upregulated to the same extent for all genes tested (Figure 9).
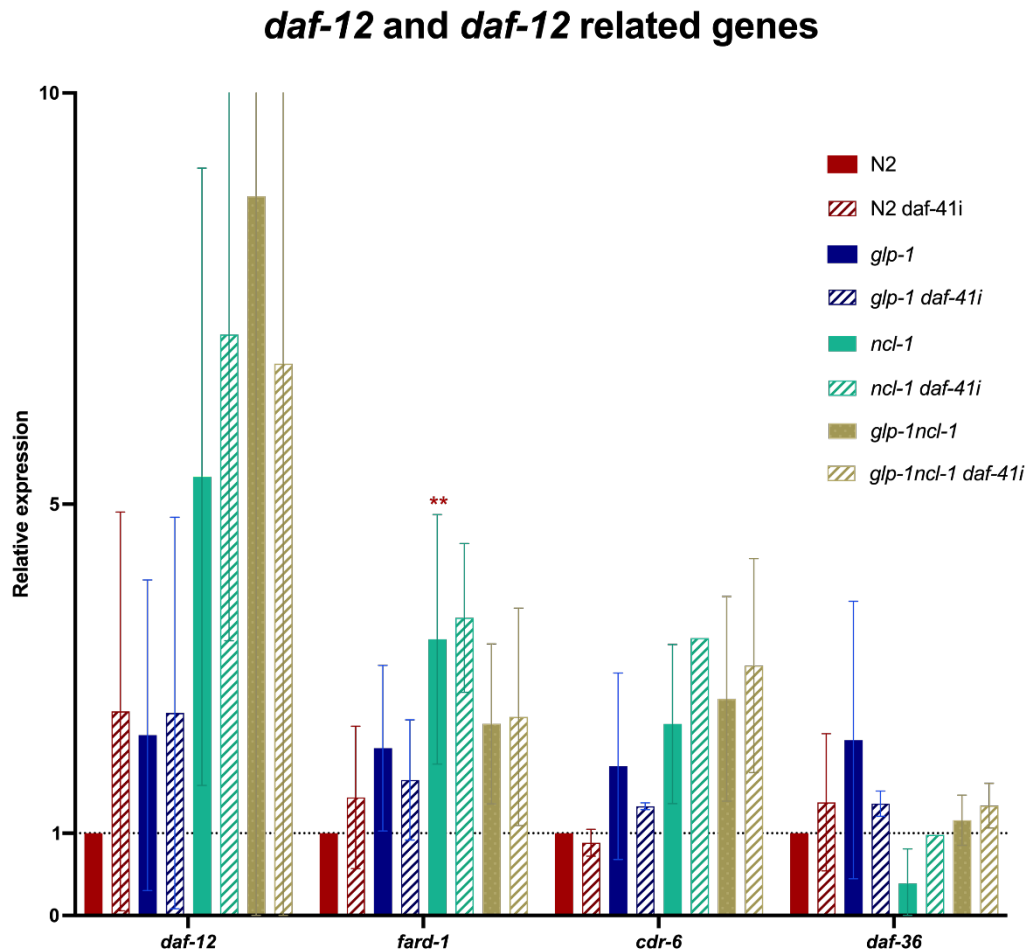

Figure 9. Relative gene expression of daf-12 and related genes (fard-1, cdr-6, daf-36) in N2, glp-1, ncl-1, glp-1ncl-1worms with or without daf-41 downregulation and in daf-41KO mutant. Experimental strains that had daf-41 downregulated are depicted with striped pattern. umber of worms per condition N= 500, biological replicates n=8, four technical replicates. The data was statistically analysed using Ordinary one-way ANOVA analysis. **p<0.01 compared to N2. Error bars show SEM (standard error) based on fold changes across 8 biological replicates.

Again, loss of *ncl-1*, both in *ncl-1* and *glp-1ncl-1* mutant backgrounds, resulted in upregulated *daf-12* and target gene expression (*fard-1* significantly and *cdr-6*). However, *ncl-1* is the only condition that showed downregulated *daf-36*.

In conclusion, due to high standard deviations, I cannot say there is a specific gene regulation in these experimental conditions.

When talking about trends, the expression levels of *daf-16*, its target genes, and *daf-12* appear to be higher in *ncl-1* and *glp-1ncl-1* compared to N2, even when *daf-41* was downregulated. Moreover, the downregulation of *daf-41* had the most pronounced impact on the expression levels of these genes in these mutants. When comparing gene expression in N2, *glp-1*, *glp-1ncl-1* and *glp-1ncl-1 daf-41i*, there appears to be no obvious trend that could indicate a specific regulation of lifespan influenced by these genes.

4.3. Activity of Transcription Factors DAF-16 and HSF-1

Using RT-qPCR, I previously measured mRNA abundance of transcription factors DAF-16, HSF-1, and DAF-12, but their expression levels do not inform of their activity as much as the expression level of their target genes. To measure DAF-16 and HSF-1 activity, I measured the rate of their nuclear localisation and foci formation by visualizing GFP-tagged transcription factors.

4.3.1. DAF-16 Translocation

The rate of DAF-16 nuclear localisation at 25 ℃ in *daf-16::gfp*, *daf-16::gfp;glp-1*, *daf-16::gfp;glp-1ncl-1* grown on luciferase, *daf-41i*, *daf-16i* and *daf-2i* plates is shown in Figure 10 and Supplementary Table 1.
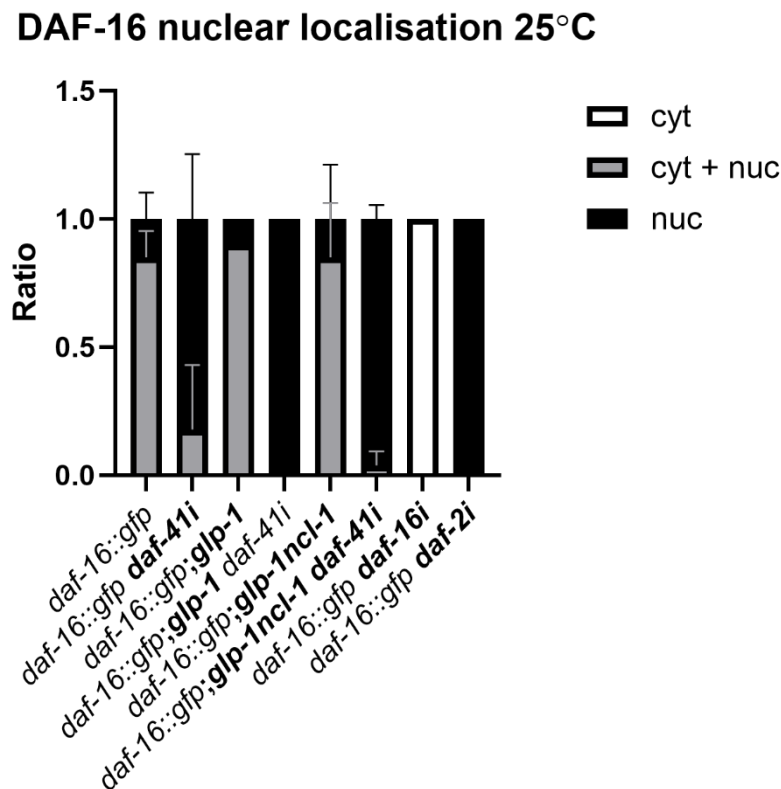

Figure 10. DAF-16::GFP localisation at 25 ℃ in DAF-16::GFP (luciferase and daf-41i), DAF-16::GFP;glp-1 (luciferase and daf-41i), DAF-16::GFP;glp-1ncl-1 (luciferase and daf-41i), DAF-16::GFP daf-16i and DAF-16::GFP daf-2i. The DAF-16 nuclear localisation is mostly both cytosolic and nuclear in DAF-16::GFP, DAF-16::GFP;glp-1 and DAF-16::GFP;glp-1ncl-1 mutants (70-90%). DAF-16::GFP localisation is mostly nuclear in strains grown on daf-41 RNAi: DAF-16::GFP daf-41i, DAF-16::GFP;glp-1 daf-41i, DAF-16::GFP;glp-1ncl-1 daf-41i (92%), and as well in the DAF-16::GFP daf-2i, a positive control (100%). The DAF-16::GFP localisation is completely cytosolic in the second control DAF-16::GFP daf-16i (100%). N = 10, n = 1-4. The data was statistically analysed using Ordinary one-way ANOVA analysis. Error bars show SEM (calculated across biological replicates).

The DAF-16 nuclear localisation is mostly both cytosolic and nuclear in *daf-16::gfp*, *daf-16::gfp;glp-1* and *daf-16::gfp;glp-1ncl-1* mutants (70-90%). DAF-16::GFP localisation is mostly nuclear in strains grown on *daf-41* RNAi: *daf-16::gfp daf-41i*, *daf-16::gfp;glp-1*

daf-41i, *daf-16::gfp;glp-1ncl-1 daf-41i* (92%), and as well in the *daf-16::gfp daf-2i,* a positive control (100%). Finally, the *daf-16::gfp* localisation is completely cytosolic in the second control *daf-16::gfp daf-16i (100%)*.

The exposure to 37 ºC induced a much stronger GFP signal and its localisation was nuclear in all strains except *daf-16::gfp daf-16i* control which only had cytosolic expression (Figure 11).
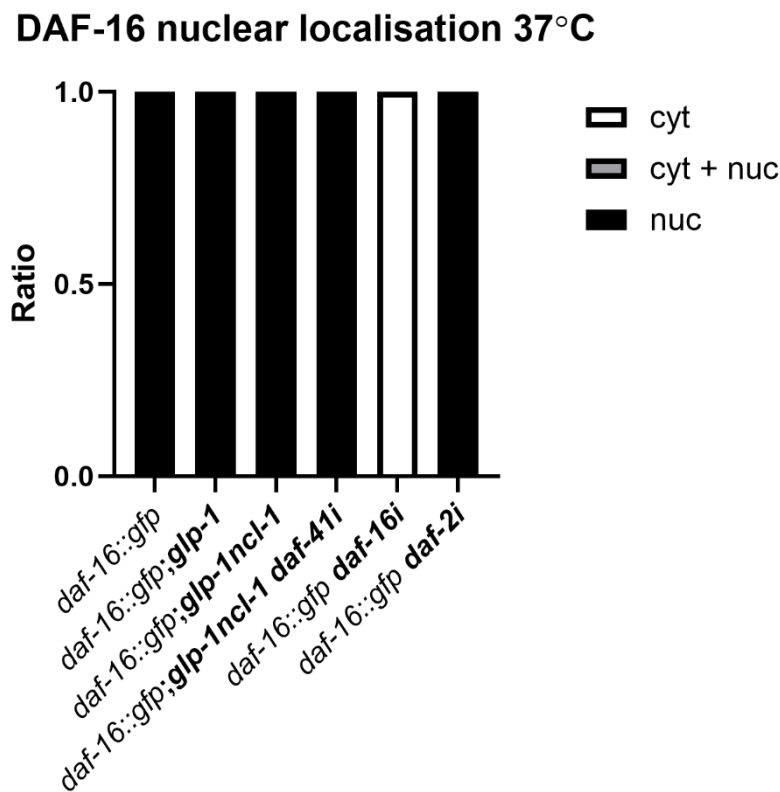
Figure 11. DAF-16::GFP localisation at 37 ºC in daf-16::gfp (luciferase and daf-41i), daf-16::gfp;glp-1 (luciferase and daf-41i), daf-16::gfp;glp-1ncl-1 (luciferase and daf-41i), daf-16::gfp daf-16i and daf-16::gfp daf-2i. DAF-16::GFP localisation was nuclear in all of the strains except in the daf-16::gfp daf-16i strain. N = 10, n = 3.

4.3.2. HSF-1 Foci Formation

To see if *daf-41* downregulation influences HSF-1 activity, I measured the ratio of tail hypodermal cells that had HSF-1 foci compared to the total cell number at 25 ºC. The results are shown in Figure 12 and Supplementary Table 2. The results indicate that **daf-41 downregulation increased the HSF-1 activity** as there was a significantly higher percentage of HSF-1 foci-positive nuclei in *hsf-1::gfp daf-41i* worms compared to *hsf-1::gfp*.

To see if *daf-41* downregulation influences HSF-1 foci formation at higher temperatures in different mutant backgrounds, the same experiment was done after a 30-minute exposure to 37 ºC.
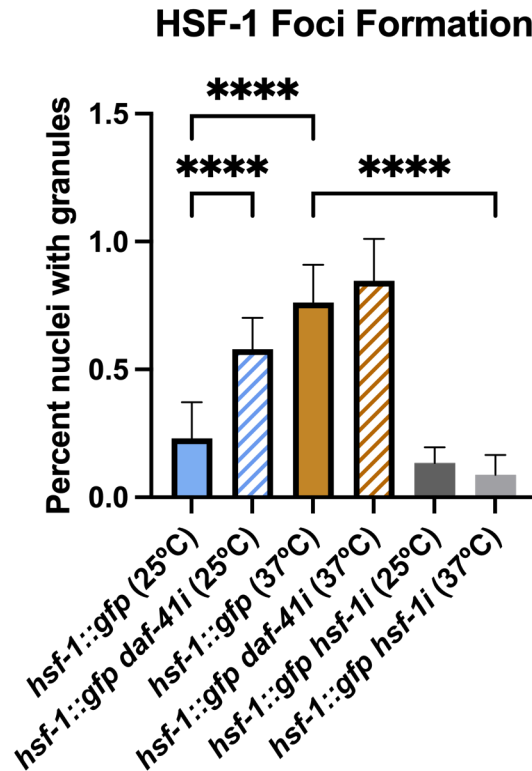

Figure 12. HSF-1 *nuclear foci formation in hsf-1::gfp, hsf-1::gfp daf-41i and hsf-1::gfp hsf-1i worms at 25 ºC and after 30-min 37 ºC exposure. Experimental strains that had daf-41 downregulated are depicted with striped patterns. At 25 ºC, there was a significantly higher percentage of* HSF-1 *foci-positive nuclei in hsf-1::gfp daf-41i worms compared to hsf-1::gfp. hsf-1::gfp worms incubated at 37 ºC had a significantly higher percentage of* HSF-1 *foci-positive cells compared to hsf-1::gfp worms kept at 25 ºC. Moreover, hsf-1::gfp daf-41i worms exposed to 37 ºC had a significantly higher percentage of* HSF-1 *foci-positive cells than hsf-1::gfp daf-41i worms kept at 25 ºC. 25 ºC hsf-1::gfp hsf-1i control did not have a significantly lower percentage of* HSF-1 *foci compared to 25 ºC hsf-1::gfp, but hsf-1::gfp hsf-1i incubated at 37 ºC compared to the 37 ºC hsf-1::gfp did. The data was statistically analysed using Ordinary one-way ANOVA. N = 10, n = 2. Error bars show SEM. ****p<0.0005*

This led to nuclear HSF-1 foci formation in almost all the cells in all conditions. *hsf-1::gfp* worms incubated at 37 ºC had a significantly higher percentage of HSF-1 foci-positive cells compared to *hsf-1::gfp* worms kept at 25 ºC (Figure 12). Moreover, *hsf-1::gfp daf-41i* worms exposed to 37 ºC had a significantly higher percentage of HSF-1 foci-positive cells than

hsf-1::gfp worms kept at 25 ºC. As a control I used *hsf-1i*, and it shows significantly lowered amount of foci formation at 37 °C.

4.4. Stress Resistance

As *daf-41* downregulation partially restored *glp-1ncl-1* lifespan, I wanted to see if this is followed by a change in worm resistance to heat and oxidative stress.

4.4.1. Heat Stress Resistance

N2, *daf-41*, *glp-1*, *ncl-1* and *glp-1ncl-1* grown on luciferase and *daf-41i* plates were exposed to heat stress (incubation at 37 ºC) and their survival was scored across the span of two hours (Figure 13).
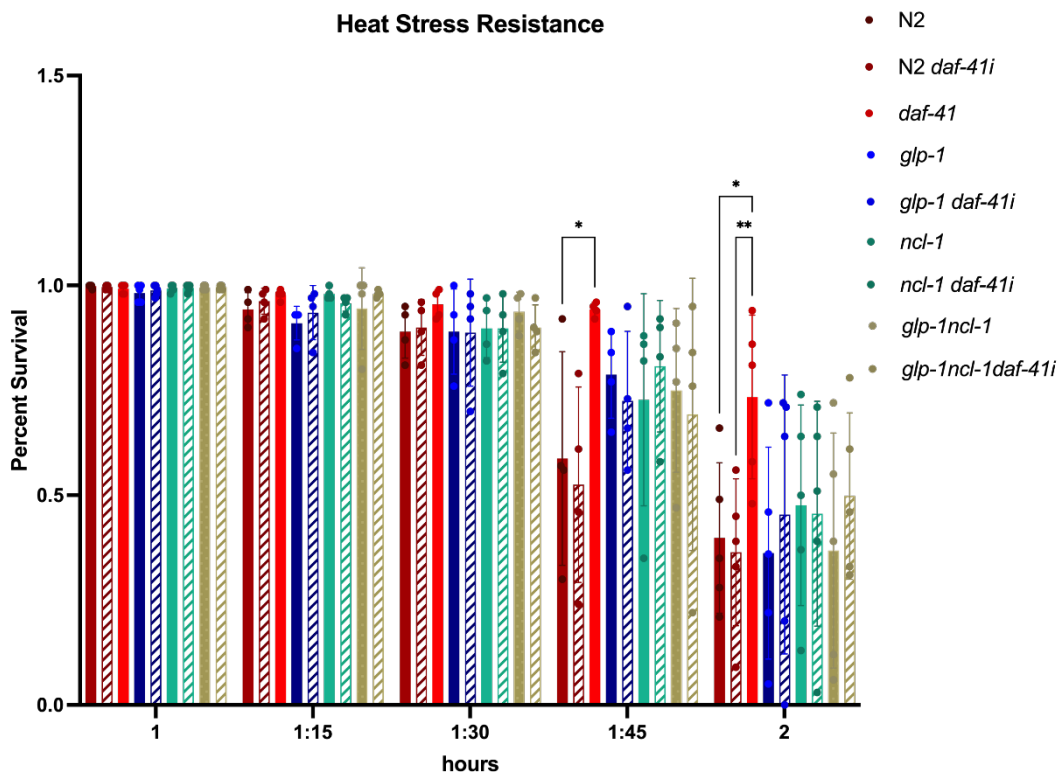
Figure 13. Worm resistance to 1, 1:15, 1:45 and 2-hour exposure to heat stress. The worms were incubated at 37 ºC for various lengths of time after their percent of survival was calculated. The figure shows the survival percentage of N2, glp-1, glp-1ncl-1, glp-1ncl-1 daf-41i and daf-41 worms. Across all time points, daf-41 knockdown significantly increased N2 thermotolerance, while daf-41 downregulation slightly decreased worm thermotolerance. Glp-1 had higher thermotolerance than N2 at 1:45, but slightly lower at 2:00. Loss of ncl-1 followed a similar trend in both mutant backgrounds (ncl-1, glp-1ncl-1). N = 200 n = 4-5. Data was analyzed using the Ordinary two-way ANOVA test. *p<0.05, **p<0.01

No significant differences exist in the heat stress resistance among all the experimental groups after 1, 1:15, and 1:30 hour exposure to heat stress. Although the results are highly variable, and there are not many significant differences in the heat stress resistance among mutants at 1:45 and 2:00, some trends can be observed.

daf-41 knockout mutant had an increased thermotolerance compared to N2, while *daf-41* downregulated mutant had a slightly decreased thermotolerance compared to N2. There are no specific trends regarding the effects of *daf-41* downregulation in mutants.

4.4.2. Oxidative Stress Resistance

Daf-41 downregulation did not significantly influence worm survival after 3-hour exposure to 100 mmol/dm^3 (mM) paraquat (Figure 14).

Figure 14. Worm resistance to 100 mM paraquat 3-hour exposure. The figure shows the survival percentage of N2, glp-1, ncl-1, glp-1ncl-1 (grown on luciferase and daf-41i), daf-2 and clk-1 worms after a 3-hour exposure to 100 mM paraquat. Experimental strains that had daf-41 downregulated are depicted with striped patterns. There is no significant difference in survival between groups. There appears to be a trend where daf-41 downregulation decreases worm survival (except in glp-1ncl-1 where it increases survival). Daf-2 and clk-1 worms have a higher resistance to 10 mM paraquat compared to N2. N = 30, n = 2-3 Data was analysed using the Ordinary one-way ANOVA test. Error bars show SEM.

Moreover, there is no significant difference in paraquat resistance in *glp-1* and *glp-1ncl-1* worms compared to the wildtype N2. It is important to note that data show high variability among replicates and that *clk-1* mutants have much higher resistance to paraquat-induced stress, a control that according to literature has a lower oxidative stress resistance compared to N2 worms (Schaar et al., 2015). *Daf-2* worms had the highest resistance to oxidative stress.

I also looked if *daf-41* downregulation influenced worm resistance to oxidative stress induced by 10 mM and 20 mM hydrogen peroxide (H_2O_2). After 3h exposure to 10 mM H_2O_2, only *daf-2 (*control*)* showed a significant increase in their resistance to oxidative stress compared to N2 (Figure 15). *clk-1* (second control) had a similar resistance to N2.

H_2O_2 10 mM

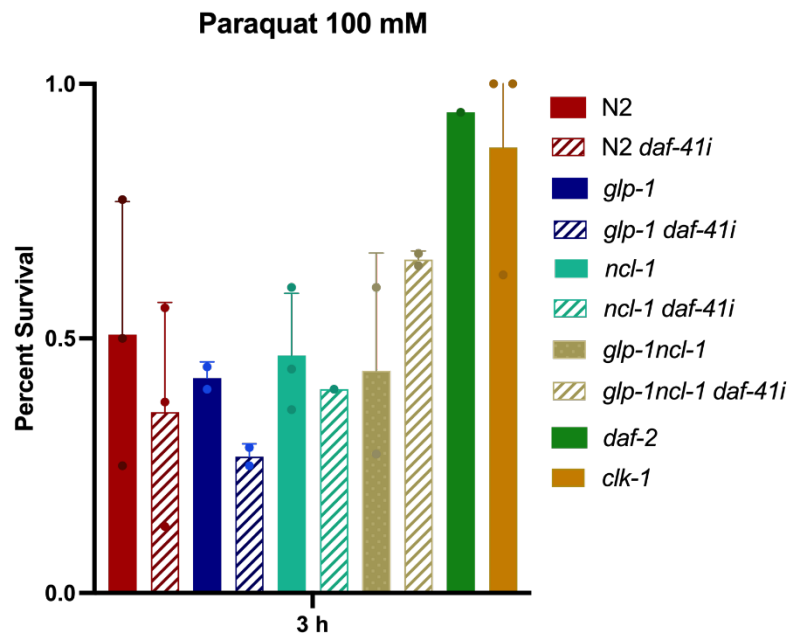*Figure 15. Worm resistance to 10 mM H_2O_2 3-hour exposure. The figure shows the survival percentage of N2, glp-1, ncl-1, glp-1ncl-1 (grown on luciferase and daf-41i), daf-2 and clk-1 worms after a 3-hour exposure to 10 mM H_2O_2. Experimental strains that had daf-41 downregulated are depicted with striped patterns. There is no significant difference in worm survival between groups except in daf-2 worms which had a significantly increased resistance than N2. Clk-1 worms had similar resistance to N2. Data was analysed using the Ordinary one-way ANOVA test. ****p<0.0001 N = 30, n = 1- 2. Error bars show SEM.*

One hour of exposure to 20 mM H_2O_2 did not significantly influence worm survival except in *glp-1ncl-1* mutants (Figure 16). Downregulation of *daf-41* significantly increased *glp-1ncl-1* survival after 1-hour exposure to 20 mM H_2O_2 stress but did not show any influence after 2-hour exposure. 3-hour-exposure even decreased *glp-1ncl-1daf-41i* survival.
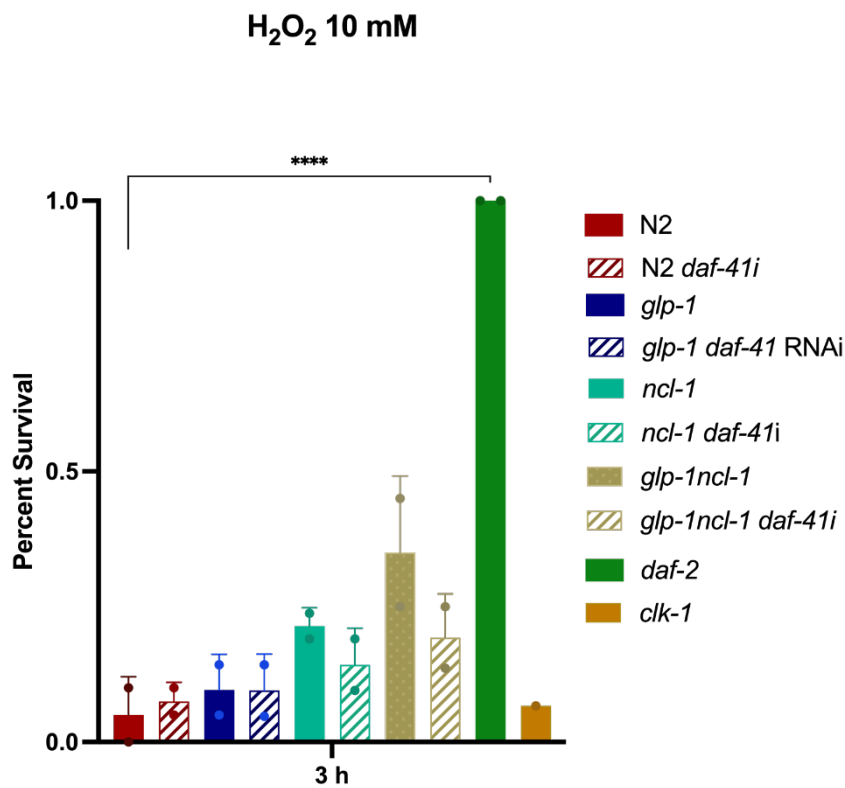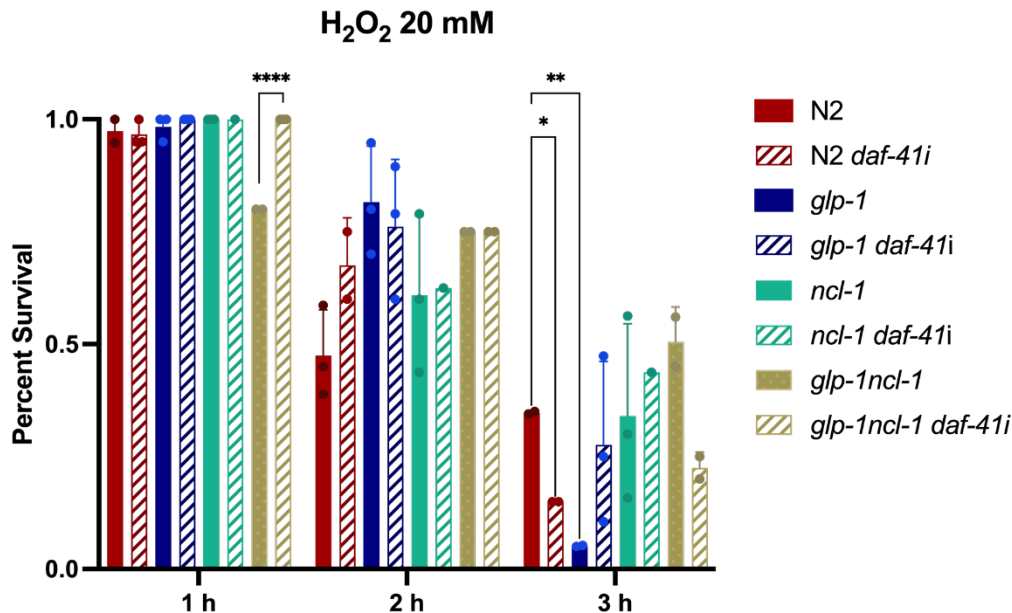

Figure 16. Worm resistance to 20 mM H_2O_2 1-, 2- and 3-hour exposure. The figure shows the survival percentage of N2, glp-1, ncl-1, glp-1ncl-1 (grown on luciferase and daf-41i) worms after a 3-hour exposure to 20 mM H_2O_2. Experimental strains that had daf-41 downregulated are depicted with striped patterns. 1-hour 20 mM H_2O_2 exposure only significantly reduced survival in glp-1ncl-1 worms. 2-hour 20 mM H_2O_2 exposure decreased worm survival to a similar extent in all conditions. 3-hour 20 mM H_2O_2 exposure further decreased worm survival. Daf-41 downregulation in N2 worms significantly decreased their survival percentage at that time point. Moreover, glp-1 survival was also significantly decreased compared to N2 at three-hour point. Data was analysed using the Ordinary two-way ANOVA test. *p<0.05, **p<0.01, ****p<0.0001 N = 30, n = 2-3. Error bars show SEM.

Two-hour exposure to 20 mM H_2O_2 decreased worm survival to a similar extent in all the strains, resulting in no significant differences among groups.

daf-41 downregulation in N2 worms significantly decreased N2 worm survival after three-hour exposure to 20 mM H_2O_2. Moreover, *glp-1* worms also had a significantly lower resistance to three-hour 20 mM H_2O_2 oxidative stress compared to N2. Although not significant at this time point, *glp-1ncl-1* worms had the higher percentage of survival compared to *glp-1* and similar to the one of N2 worms.to N2. Finally, *daf-41* downregulation in *glp-1ncl-1* worms decreased

their resistance to oxidative stress, so the percentage of survival reverts closer to the value of *glp-1* worms.

5. Discussion

Previous work in the Antebi laboratory established *ncl-1* as a regulator of major longevity pathways including dietary restriction (DR) and insulin/IGF-1 signalling pathway (Tiku et al., 2017). They went further to elucidate potential downstream effectors of *ncl-1* through an RNAi screen, from which they identified *daf-41*/p23 as an interesting candidate. Its downregulation was able to partially rescue lifespan in *glp-1ncl-1* and *raga-1ncl-1* mutants.

daf-41 - prostaglandin E3 synthase is an HSP-90 co-chaperone (Horikawa et al., 2015) and is known to regulate *C. elegans* lifespan in a temperature-dependent manner. *C. elegans* has different lifespan lengths at different temperatures, at 20 ºC, a usual cultivating temperature, it lives approximately three weeks, at higher temperatures (25 ºC) around ten days shorter and at lower temperatures (15 ºC) around ten days longer. At warm temperatures (25 ºC), *daf-41* limits lifespan, whereas at cold temperatures (15 ºC) it promotes longevity (Horikawa et al., 2015). At warm temperatures, *daf-41* activates insulin/IGF-1 signalling through *daf-16*/FOXO and heat shock signalling through *hsf-1*, while at colder temperatures mechanism of its activity depends on insulin/IGF-1 through *daf-16* and steroidal *daf-12*/FXR signalling. However, the molecular mechanisms by which *daf-41* regulates lifespan in *glp-1ncl-1* mutants are still unclear.

The primary objective of this research project was to characterize the mechanism by which DAF-41 extends the lifespan of the *glp-1ncl-1* strain of *C. elegans*. This was accomplished by investigating whether the insulin/IGF-1 signalling pathway genes, heat shock response genes, and steroid signalling pathway genes are involved and whether the presence of DAF-41 is necessary for the regulation of tolerance to elevated temperature and oxidative stress via NCL-1.

5.1. The Lifespan Method

To determine an appropriate lifespan method, I measured lifespan in N2 and *raga-1* worms using the FUdR and transfer method. Lifespan results indicate that the method significantly impacts the lifespan results. The FUdR treatment resulted in a significantly shorter lifespan of N2 and *raga-1* worms compared to the transfer method. This is consistent with the literature as

Anderson and colleagues in 2016 observed that FUdR influences lifespan length in some genotypes through activation of the stress response. Moreover, *raga-1* mutants lived longer compared to N2, which is also consistent with previous findings (Zhang et al., 2019). The main limitation of this experiment was the small experimental number of *raga-1* worms. This was due to the fact that *raga-1* mutants have a decreased number of progeny, and this was not taken in account when preparing this experimental group. Finally, only one biological replicate was tested.

5.2. Lifespan

To see how *daf-41* downregulation influences *glp-1ncl-1* lifespan, and to gain more insight in *daf-41* influence on worm lifespan, I performed lifespan experiments with wildtype N2 worms, *glp-1*, *ncl-1*, *glp-1ncl-1* and *daf-41* mutants, both on luciferase and *daf-41* RNAi plates. *daf-41* downregulation in *glp-1ncl-1* worms partially rescued *glp-1* longevity and increased *glp-1ncl-1* median lifespan by 11%. This is a more subtle lifespan rescue compared to the unpublished laboratory data where *daf-41* downregulation increased median lifespan by 30%. As *daf-41* downregulation did not significantly influence the lifespan of *ncl-1* and *glp-1* worms alone, it seems that this effect of *daf-41* on worm lifespan is specific for *glp-1ncl-1* double mutants. Moreover, consistent with the literature, *glp-1* worms lived significantly longer than N2 (Lee et al., 2019), while *ncl-1* mutants had a significantly shorter median (by 10%) and maximum lifespan (by 22%) (Tiku et al., 2017).

Regarding the *daf-41* downregulation in wildtype N2, an opposite effect was observed as it decreased median N2 lifespan by 30%. Previous work from Horikawa and co-workers in 2015 established *daf-41* as a temperature-dependant regulator of *C. elegans* lifespan as its loss extended lifespan at 25 ºC and shortened at 15 ºC compared to WT, while not influencing lifespan at the usual growing temperature of 20 ºC. Contrary to this, in the lifespan experiments I performed; at 20 ºC *daf-41* mutant lived shorter compared to wildtype. *daf-41* downregulation in N2 worms had the same effect as *daf-41* KO on worm lifespan, as they had the same median lifespan (14 days) and similar maximum lifespan (*daf-41* = 14.4 days, N2 *daf-41i* = 14.7 days). These data suggest that *daf-41* downregulation has the same effect on *C. elegans* lifespan as *daf-41* knock-out mutation. Moreover, the fact that *daf-41* downregulation in *glp-1ncl-1* worms

partially rescued their lifespan indicates a temperature-independent role of *daf-41* in *C. elegans* regulation of lifespan.

Interestingly, Horikawa observed that at 25 °C, *daf-41* mutants lived longer compared to WT, whilst I observed that *daf-41* developed at 25 °C and lived as an adult at 20 °C, not only lived the same as WT at that temperature but lived shorter compared to WT. One potential reason for the difference in lifespan length of *daf-41* mutants in mine and Horikawa's experiments could be the different temperatures during worm larval development and adult life. Horikawa and colleagues kept *daf-41* mutants at the same temperature throughout their development and adult life, whilst I developed worms at 25 °C and after they reached adulthood, kept them in a 20 °C incubator. I did it that way to keep the same conditions for all experimental strains, including temperature-sensitive *glp-1* which had to be developed at 25 °C to express its phenotype. This suggests that different temperature during larval development and adult life influences DAF-41 mediated regulation of *C. elegans* lifespan. It would not be surprising as it was already shown that temperature during larval development influences *C. elegans* lifespan through DAF-16/FOXO signaling (Zhang et al., 2015). Larval exposure during development to 25 °C has been shown to increase WT lifespan. Maybe this increase is dependent on DAF-41 as well and could explain the shorter lifespan of *daf-41* mutants.

The main drawback of lifespan experiments is the fact that, due to time constraints, it was done only in one biological replicate.

5.3. Relative Gene Expression

When testing primer efficiency, all primers had an efficiency close to 100%, but the *daf-12* primer did not amplify any DNA at all. For this reason, I generated my own *daf-12* primer sequences (but could not measure their efficiency). To test the potential signalling mechanism underlying *daf-41* partial lifespan rescue in *glp-1ncl-1* mutants, using RT-qPCR I measured relative gene expression in N2, *glp-1*, *ncl-1* and *glp-1ncl-1* (*luci* and *daf-41i*). As Horikawa et al. (2015) previously observed *daf-41* influences *C. elegans* lifespan through insulin/IGF-1, heat shock and steroidal signalling pathway, I measured relative expression of *daf-16,* its target genes *dod-3, lipl-4, sod-3*; *hsf-1*, *hsf-1* target genes *hsp-16.2, hsp-4, hsp-70; daf-12* and *daf-12* related genes *fard-1, cdr-6* and *daf-36*. *daf-41* downregulation did not significantly influence

the expression of most genes in any genetic background. Moreover, there is no trend in gene expression when comparing *glp-1*, *glp-1ncl-1* and *glp-1ncl-1 daf-41i* mutants.

However, there was a significant increase in *sod-3* and *fard-1* gene expression in *ncl-1* mutants. Moreover, the *dod-3*, *lipl-4* and *sod-3* (*daf-16* target genes) and *fard-1* (*daf-12* target gene) gene expression was significantly higher in *ncl-1 daf-41i* mutants compared to N2. Downregulation of *daf-41* in *glp-1ncl-1* worms resulted in the higher expression of *sod-1*, *dod-3* and *cdr-6*.

Finally, there was a significant decrease in *hsf-1* expression in *ncl-1* (both *luci* and *daf-41i*) compared to N2. Horikawa et al. (2015) observed that *daf-41* at 25 ºC had the higher relative expression of *daf-16* target genes *dod-3* and *lipl-4* compared to 20 ºC N2, whereas in my experiments N2 *daf-41i* expression of these genes did not significantly change compared to N2. In the Horikawa paper, *daf-41* expression of *hsf-1* target genes did not significantly increase compared to N2 at 25 ºC. In my experiments daf-41 downregulation in N2 did not significantly influence the expression of these genes, except of *hsp-70*. A similar lack of significant change in gene expression was observed in Horikawa's' *daf-12* and its target genes (*daf-36*, *cdr-6*, *fard-1*) at 25 ºC and in my experiments.

Although there are no significant differences in gene expression amongst mutants, there appears to be a distinct trend related to *ncl-1* loss in both *ncl-1* compared to N2 and *glp-1ncl-1* compared to *glp-1*, especially in *daf-16*, *hsf-1* and their target gene expression.

All in all, it seems that the molecular mechanism behind the lifespan extension induced by *daf-41* downregulation in *glp-1ncl-1* mutants is not regulated through heat shock (*hsf-1*), insulin/IGF-1 (*daf-16*) or steroidal (*daf-12*) signalling pathway. It is difficult to confirm this due to a very high variability among biological replicates. The potential reason for high variability is the fact that I synchronised worms with the hypochlorite treatment which does not completely synchronise the worm population. As worm life-cycle stages have different expression profiles, these differences get exacerbated after qRT-PCR. To avoid this in the future, after hypochlorite treatment, I would hand-pick the worms at the specific life stage (L4).

It is possible that DAF-41-mediated *glp-1ncl-1* lifespan extension does not involve the specific target genes chosen to represent the activity of insulin, steroid and heat-shock signalling pathways. The next step could be choosing to measure the expression of other target genes involved in this (or other) signalling pathways.

Moreover, it is necessary to measure the protein levels of these genes as gene expression often does not correlate with protein levels. This could be done by performing a western blot or by a pull-down assay to identify new *daf-41* interacting proteins.

5.4. Activity of HSF-1 and DAF-16

The mRNA expression of HSF-1 and DAF-16 transcription factors and their target genes indicates activity (or inactivity) of these pathways. But as activation of a TF and its respective signalling factors usually do not have to result in its expression levels change, I wanted to measure the activity of these TF in another way. To do this, I used the strains which had a fused TF gene with a GFP gene. This helps us visualise the active nuclear (DNA) localisation where a TF promotes gene transcription.

To measure DAF-16 activity and see if it followed the respective changes in gene expression, I measured the percentage of hypodermal tail cells that had nuclear, cytosolic or both nuclear and cytosolic DAF-16::GFP localisation, with higher nuclear localisation indicating active DAF-16, intermediate indicating partial activity and cytosolic a lack of activity. The activity of *daf-16* is higher in all strains that had *daf-41* downregulation indicating that *daf-41* inhibits *daf-16* activity. However, this is not consistent with the levels of *daf-16* and its target relative gene expression levels. Interestingly, Horikawa et al. (2015) did not observe any changes in DAF-16::GFP localisation in *daf-41* mutants compared to N2.

To see if higher temperatures influenced DAF-16 activity in different genetic backgrounds, the same experiment was performed at 37 ºC. *daf-41* downregulation, nor different genetic backgrounds, did not influence *daf-16* translocation at higher temperatures.

Unfortunately, due to time constraints, I was not able to generate *hsf-1::gfp;glp-1* and *hsf-1::gfp;glp-1ncl-1* mutants, so I measured HSF-1 foci formation only in *hsf-1::gfp* worms. The *hsf-1* mRNA expression did not vary between N2 and N2 *daf-41i*. However, to check if *daf-41* downregulation influenced HSF-1 foci formation, I measured the ratio of tail hypodermal cells that had HSF-1 foci compared to the total cell number. The results suggest that *daf-41* downregulation induced HSF-1 activity. This is partially consistent with *hsf-1* target gene expression as there was a slightly higher expression of *hsf-1* target genes *hsp-4* and *hsp-70*

in N2 *daf-41i* worms compared to N2. Interestingly, Horikawa et al. (2015) did not observe any HSF-1 foci formation in *daf-41* mutants.

To determine if *daf-41* downregulation influences HSF-1 activity in response to higher temperature exposure as well, I measured the ratio of tail hypodermal cells that had HSF-1 foci compared to total cell number after 30-minute exposure to 37 ºC. Higher temperature led to HSF-1 foci formation in almost all the cells and was not influenced by *daf-41* downregulation.

In the literature, as a positive control, *hsf-1::gfp* worms are usually exposed to 37 ºC for two minutes (Horikawa et al., 2015), but as I grew worms at a higher temperature than usual (25 ºC compared to 20 ºC), longer exposure time was required to observe the HSF-1 foci formation (30 min). This was previously observed in the literature as well (Morton & Lamitina, 2013). One crucial drawback of this is experiment is the fact that I used sodium azide for immobilisation of worms for imaging. It was shown that sodium azide can induce HSF-1 foci formation (Morton & Lamitina, 2013), so it possibly influenced the results. For this reason, in the future, I would use a different method to immobilise worms for imaging, such as cold-exposure immobilisation.

Finally, due to time restraints, only two biological replicates were tested. In the future, I would perform at least three biological replicates.

5.5 The Heat Stress Assay

N2, *glp-1*, *ncl-1*, *glp-1ncl-1* (grown on *luci* and *daf-41i*) and *daf-41* were incubated at 37 ºC across the 2 hours, through which their percentage of survival was calculated. There are no significant differences in the heat stress resistance among all the experimental groups after 1, 1:15, and 1:30-hour exposure to heat stress.

daf-41 mutants were significantly more resistant to heat stress than N2 after 1:45 and 2-hour 37 ºC incubation. This is particularly interesting as *daf-41* mutants had a shorter lifespan compared to N2, a contrary observation as lifespan length usually correlates with heat resistance (Lithgow et al., 1995). Interestingly N2 *daf-41i* worms had a slightly lower thermal resistance compared to N2, indicating that *daf-41* downregulation and knockdown differently influence heat stress resistance.

Due to the high variability of results, there is no significant difference in thermotolerance when comparing N2 with other strains, nor when comparing the strains that had *daf-41* downregulated to the ones that did not.

Hemphill et al. (2022) observed that *glp-1(e2141)* was not resistant to heat stress at the L4 stage but at the adult phase was, indicating that this strain acquires physiological properties that enable it to live longer only in adulthood. In this experiment, I used L4 *glp-1* worms, so this could explain the fact that *glp-1* worms had the lowest heat stress resistance at 1:15 at a 2-hour time point.

It seems that heat stress resistance does not always follow trends observed in lifespan length, probably due to the high variability of results, but also due to the picked life stage of experimental worms. If I had repeated the experiment, I would measure thermotolerance (and tolerance to other stressors) in more than one worm life stage, for example in L4 and adults at least.

5.6. Oxidative Stress

Three-hour exposure to 100 mM paraquat did not significantly influence the survival of any experimental strain, although the positive control *daf-2* had the highest resistance to oxidative stress. This indicates that oxidative stress resistance induced by paraquat does not correlate with lifespan length among these groups.

Moreover, 3-hour exposure to 10 mM H_2O_2 did not significantly influence worm resistance except for *glp-1ncl-1* and the positive control *daf-2* which had a significantly higher resistance to oxidative stress.

On the contrary, 1-hour-20 mM H_2O_2 exposure significantly decreased *glp-1ncl-1* survival compared to N2 and *glp-1ncl-1 daf-41i*, but did not decrease much further after 2 and 3 hours. Two-hour exposure to 20 mM H_2O_2 led to comparable decreases in worm survival across all experimental groups, resulting in no significant differences among them. Downregulation of *daf-41* in N2 worms significantly reduced their survival after a three-hour exposure to 20 mM H_2O_2. Additionally, *glp-1* worms exhibited significantly lower resistance to three-hour

exposure to 20 mM H_2O_2 oxidative stress compared to N2 worms. Unfortunately, I did not include controls for the 20 mM H_2O_2 assay.

The first step in choosing a future direction would be to generate *daf-41;glp-1* and *daf-41;glp-1ncl-1* mutants and repeat all of these experiments. This would give us more insight into the exact influence *daf-41* has on *glp-1ncl-1* strain, especially as gene downregulation and gene knock-down have different effects on worm physiology. Moreover, *daf-41* is a gene mostly expressed in worm neurons (Horikawa et al., 2015). This probably leads to high variability in my results as it is known that RNA inhibition in worms by feeding downregulates genes in the brain with less efficiency (Timmons et al., 2001). Finally, one should do experiments in multiple worm life stages, at least one in the larval and one in the adult stage, as it is known this could largely influence worm resistance to various stressors.

6. Conclusion

I confirmed the previous observation in the laboratory that the downregulation of *daf-41* in *glp-1ncl-1* mutants partially rescues the longevity of *glp-1* worms. This influence appears to be specific to the *glp-1ncl-1* mutants, and not observed in *glp-1* or *ncl-1* strains. Moreover, this suggests that *daf-41* regulates *C. elegans* lifespan in a previously unknown, temperature-independent manner. However, relative gene expression did not significantly differ among these groups, which makes it difficult to pinpoint the exact signalling pathway involved in this lifespan regulation. Relative gene expression is a sensitive and variable measure, so analysing these genes at the protein level may provide more conclusive insights. There is a slight indication that the partial lifespan rescue of *glp-1ncl-1* worms by *daf-41* downregulation may involve inhibition of the DAF-16 transcription factor, as it was more active in *daf-16::gfp*;*glp-1ncl-1 daf-41*i than in *daf-16::gfp*;*glp-1ncl-1* mutants. Finally, there is no correlation between the lifespan length of *glp-1*, *glp-1ncl-1*, and *glp-1ncl-1 daf-41i* worms and their resistance to heat or oxidative stress induced by paraquat or H_2O_2.

Contrary to previous findings, *daf-41* and N2 *daf-41*i worms lived significantly shorter than N2, suggesting a similar mechanism of *daf-41* knockout and knockdown. This implication was refuted by further experiments showing that *daf-41* knockdown and knockout worms responded differently to heat stress. This highlights the importance of replicating these experiments in *glp-1*;*daf-41* and *glp-1ncl-1*;*daf-41* mutants, especially considering that *daf-41* is primarily expressed in neurons, where RNA interference appears to be less effective.

Furthermore, *daf-41* downregulation across all strains did not significantly influence relative gene expression, thermotolerance, or oxidative stress resistance. However, transcription factor activity assays indicate that *daf-41* inhibited *daf-16* and *hsf-1* in all conditions.

To conclude, *daf-41* downregulation partially restores *glp-1ncl-1* longevity without influencing stress tolerance, but likely through a DAF-16 and HSF-1-dependent mechanism.

7. Literature

Anderson, E. N., Corkins, M. E., Li, J.-C., Singh, K., Parsons, S., Tucey, T. M., Sorkaç, A., Huang, H., Dimitriadi, M., Sinclair, D. A., & Hart, A. C. (2016). *C. elegans* lifespan extension by osmotic stress requires FUdR, base excision repair, FOXO, and sirtuins. *Mechanisms of Ageing and Development*, *154*, 30–42. https://doi.org/10.1016/j.mad.2016.01.004

Antebi, A. (2013). Steroid Regulation of *C. elegans* Diapause, Developmental Timing, and Longevity. In A. E. Rougvie & M. B. O'Connor (Eds.), *Current Topics in Developmental Biology* (Vol. 105, pp. 181–212). Academic Press. https://doi.org/10.1016/B978-0-12-396968-2.00007-5

Ben-Zvi, A., Miller, E. A., & Morimoto, R. I. (2009). Collapse of proteostasis represents an early molecular event in *Caenorhabditis elegans* aging. *Proceedings of the National Academy of Sciences*, *106*(35), 14914–14919. https://doi.org/10.1073/pnas.0902882106

Biebl, M. M., Lopez, A., Rehn, A., Freiburger, L., Lawatscheck, J., Blank, B., Sattler, M., & Buchner, J. (2021). Structural elements in the flexible tail of the co-chaperone p23 coordinate client binding and progression of the Hsp90 chaperone cycle. *Nature Communications*, *12*(1), 828. https://doi.org/10.1038/s41467-021-21063-0

C. elegans Sequencing Consortium. (1998). Genome sequence of the nematode *C. elegans:* A platform for investigating biology. *Science (New York, N.Y.)*, *282*(5396), 2012–2018. https://doi.org/10.1126/science.282.5396.2012

Campisi, J., Kapahi, P., Lithgow, G. J., Melov, S., Newman, J. C., & Verdin, E. (2019). From discoveries in ageing research to therapeutics for healthy ageing. *Nature*, *571*(7764), 183–192. https://doi.org/10.1038/s41586-019-1365-2

Chalfie, M., Tu, Y., Euskirchen, G., Ward, W. W., & Prasher, D. C. (1994). Green fluorescent protein as a marker for gene expression. *Science (New York, N.Y.)*, *263*(5148), 802–805. https://doi.org/10.1126/science.8303295

Chen, S., Wu, Y., Gao, Y., Wu, C., Wang, Y., Hou, C., Ren, M., Zhang, S., Zhu, Q., Zhang, J., Yao, Y., Huang, M., Qi, Y. B., Liu, X.-S., Horng, T., Wang, H., Ye, D., Zhu, Z., Zhao, S., & Fan, G. (2023). Allosterically inhibited PFKL via prostaglandin E2 withholds glucose metabolism and ovarian cancer invasiveness. *Cell Reports*, *42*(10), 113246. https://doi.org/10.1016/j.celrep.2023.113246

Chew, Y. L., Walker, D. S., Towlson, E. K., Vértes, P. E., Yan, G., Barabási, A.-L., & Schafer, W. R. (2017). Recordings of *Caenorhabditis elegans* locomotor behaviour following targeted ablation of single motorneurons. *Scientific Data*, *4*(1), 170156. https://doi.org/10.1038/sdata.2017.156

Corsi, A. K., Wightman, B., & Chalfie, M. (2015b). A Transparent window into biology: A primer on *Caenorhabditis elegans*. *WormBook: The Online Review of C. Elegans Biology*, 1–31. https://doi.org/10.1895/wormbook.1.177.1

Culetto, E., & Sattelle, D. B. (2000). A role for *Caenorhabditis elegans* in understanding the function and interactions of human disease genes. *Human Molecular Genetics*, *9*(6), 869–877. https://doi.org/10.1093/hmg/9.6.869

Denzel, M. S., Lapierre, L. R., & Mack, H. I. D. (2019). Emerging topics in *C. elegans* aging research: Transcriptional regulation, stress response and epigenetics. *Mechanisms of Ageing and Development*, *177*, 4–21. https://doi.org/10.1016/j.mad.2018.08.001

Dilberger, B., Baumanns, S., Schmitt, F., Schmiedl, T., Hardt, M., Wenzel, U., & Eckert, G. P. (2019). Mitochondrial oxidative stress impairs energy metabolism and reduces stress resistance and longevity of *C. elegans*. *Oxidative Medicine and Cellular Longevity*, *2019*(1), 6840540. https://doi.org/10.1155/2019/6840540

Fire, A., Xu, S., Montgomery, M. K., Kostas, S. A., Driver, S. E., & Mello, C. C. (1998). Potent and specific genetic interference by double-stranded RNA in *Caenorhabditis elegans*. *Nature*, *391*(6669), 806–811. https://doi.org/10.1038/35888

Folick, A., Oakley, H. D., Yu, Y., Armstrong, E. H., Kumari, M., Sanor, L., Moore, D. D., Ortlund, E. A., Zechner, R., & Wang, M. C. (2015). Lysosomal signaling molecules regulate longevity in *Caenorhabditis elegans*. *Science (New York, N.Y.)*, *347*(6217), 83–86. https://doi.org/10.1126/science.1258857

Freeman, B. C., Toft, D. O., & Morimoto, R. I. (1996). Molecular Chaperone machines: chaperone activities of the cyclophilin Cyp-40 and the steroid aporeceptor-associated protein p23. *Science*, *274*(5293), 1718–1720. https://doi.org/10.1126/science.274.5293.1718

Friedman, D. B., & Johnson, T. E. (1988). A mutation in the age-1 gene in *Caenorhabditis elegans* lengthens life and reduces hermaphrodite fertility. *Genetics*, *118*(1), 75–86. https://doi.org/10.1093/genetics/118.1.75

Garigan, D., Hsu, A.-L., Fraser, A. G., Kamath, R. S., Ahringer, J., & Kenyon, C. (2002). Genetic analysis of tissue aging in *Caenorhabditis elegans*: A role for heat-shock factor and bacterial proliferation. *Genetics*, *161*(3), 1101–1112. 10.1093/genetics/161.3.1101

Golden, J. W., & Riddle, D. L. (1984). The *Caenorhabditis elegans* dauer larva: Developmental effects of pheromone, food, and temperature. *Developmental Biology*, *102*(2), 368–378. https://doi.org/10.1016/0012-1606(84)90201-X

Goudeau, J., Bellemin, S., Toselli-Mollereau, E., Shamalnasab, M., Chen, Y., & Aguilaniu, H. (2011). Fatty acid desaturation links germ cell loss to longevity through NHR-80/HNF4 in *C. elegans*. *PLOS Biology*, *9*(3), e1000599. https://doi.org/10.1371/journal.pbio.1000599

Hansen, M., Hsu, A.-L., Dillin, A., & Kenyon, C. (2005). New genes tied to endocrine, metabolic, and dietary regulation of lifespan from a *Caenorhabditis elegans* genomic RNAi screen. *PLOS Genetics*, *1*(1), e17. https://doi.org/10.1371/journal.pgen.0010017

Hemphill, C., Pylarinou-Sinclair, E., Itani, O., Scott, B., Crowder, C. M., & Gilst, M. R. V. (2022). Daf-16 mediated repression of cytosolic ribosomal protein genes facilitates a hypoxia sensitive to hypoxia resistant transformation in long-lived germline mutants. *PLOS Genetics*, *18*(5), e1009672. https://doi.org/10.1371/journal.pgen.1009672

Hodgkin, J. (2001). What does a worm want with 20,000 genes? *Genome Biology*, *2*(11), comment2008.1-comment2008.4.

Horikawa, M., Sural, S., Hsu, A.-L., & Antebi, A. (2015). Co-chaperone p23 regulates *C. elegans* lifespan in response to temperature. *PLOS Genetics*, *11*(4), e1005023. https://doi.org/10.1371/journal.pgen.1005023

Hsin, H., & Kenyon, C. (1999). Signals from the reproductive system regulate the lifespan of *C. elegans*. *Nature*, *399*(6734), Article 6734. https://doi.org/10.1038/20694

Ji, P., Li, H., Jin, Y., Peng, Y., Zhao, L., & Wang, X. (2022). *C. elegans* as an in vivo model system for the phenotypic drug discovery for treating paraquat poisoning. *PeerJ*, *10*, e12866. https://doi.org/10.7717/peerj.12866

Kaletta, T., & Hengartner, M. O. (2006). Finding function in novel targets: *C. elegans* as a model organism. *Nature Reviews Drug Discovery*, *5*(5), 387–399. https://doi.org/10.1038/nrd2031

Kim, J. H., Jeong, H. D., Song, M. J., Lee, D. H., Chung, J. H., & Lee, S.-T. (2022). SOD3 Suppresses the Expression of MMP-1 and Increases the Integrity of Extracellular Matrix in Fibroblasts. *Antioxidants*, *11*(5). https://doi.org/10.3390/antiox11050928

Klass, M. R. (1977). Aging in the nematode *Caenorhabditis elegans*: Major biological and environmental factors influencing life span. *Mechanisms of Ageing and Development*, *6*, 413–429. https://doi.org/10.1016/0047-6374(77)90043-4

Knoblauch, R., & Garabedian, M. J. (1999). Role for Hsp90-associated cochaperone p23 in estrogen receptor signal transduction. *Molecular and Cellular Biology*, *19*(5), 3748–3759. 10.1128/mcb.19.5.3748

Lazaro-Pena, M. I., Ward, Z. C., Yang, S., Strohm, A., Merrill, A. K., Soto, C. A., & Samuelson, A. V. (2022a). HSF-1: Guardian of the proteome through integration of longevity signals to the proteostatic network. *Frontiers in Aging*, *3*. https://www.frontiersin.org/articles/10.3389/fragi.2022.861686

Lazaro-Pena, M. I., Ward, Z. C., Yang, S., Strohm, A., Merrill, A. K., Soto, C. A., & Samuelson, A. V. (2022b). HSF-1: Guardian of the proteome through integration of longevity signals to the proteostatic network. *Frontiers in Aging*, *3*. https://www.frontiersin.org/articles/10.3389/fragi.2022.861686

Lee, S.-J., & Kenyon, C. (2009). Regulation of the longevity response to temperature by thermosensory neurons in *Caenorhabditis elegans*. *Current Biology*, *19*(9), 715–722. https://doi.org/10.1016/j.cub.2009.03.041

Libina, N., Berman, J. R., & Kenyon, C. (2003). Tissue-specific activities of *C. elegans* DAF-16 in the regulation of lifespan. *Cell*, *115*(4), 489–502. https://doi.org/10.1016/S0092-8674(03)00889-4

Lin, K., Dorman, J. B., Rodan, A., & Kenyon, C. (1997). Daf-16: an HNF-3/forkhead family member that can function to double the life-span of *Caenorhabditis elegans*. *Science*, *278*(5341), 1319–1322. https://doi.org/10.1126/science.278.5341.1319

Lithgow, G. J., White, T. M., Melov, S., & Johnson, T. E. (1995). Thermotolerance and extended life-span conferred by single-gene mutations and induced by thermal stress. *Proceedings of the National Academy of Sciences*, *92*(16), 7540–7544. https://doi.org/10.1073/pnas.92.16.7540

Liu, J., Zhang, B., Lei, H., Feng, Z., Liu, J., Hsu, A.-L., & Xu, X. Z. S. (2013). Functional aging in the nervous system contributes to age-dependent motor activity decline in *C. elegans*. *Cell Metabolism*, *18*(3), 392–402. https://doi.org/10.1016/j.cmet.2013.08.007

Martínez, G., Duran-Aniotz, C., Cabral-Miranda, F., Vivar, J. P., & Hetz, C. (2017). Endoplasmic reticulum proteostasis impairment in aging. *Aging Cell*, *16*(4), 615–623. https://doi.org/10.1111/acel.12599

Morran, L. T., Cappy, B. J., Anderson, J. L., & Phillips, P. C. (2009). Sexual partners for the stressed: facultative outcrossing in the self-fertilizing nematode *Caenorhabditis elegans*. *Evolution*, *63*(6), 1473–1482. https://doi.org/10.1111/j.1558-5646.2009.00652.x

Morton, E. A., & Lamitina, T. (2013). *Caenorhabditis elegans* HSF-1 is an essential nuclear protein that forms stress granule-like structures following heat shock. *Aging Cell*, *12*(1), 112–120. https://doi.org/10.1111/acel.12024

Motola, D. L., Cummins, C. L., Rottiers, V., Sharma, K. K., Li, T., Li, Y., Suino-Powell, K., Xu, H. E., Auchus, R. J., Antebi, A., & Mangelsdorf, D. J. (2006). Identification of ligands for DAF-12 that govern dauer formation and reproduction in *C. elegans*. *Cell*, *124*(6), 1209–1223. https://doi.org/10.1016/j.cell.2006.01.037

Noddings, C. M., Wang, R. Y.-R., Johnson, J. L., & Agard, D. A. (2022). Structure of Hsp90–p23–GR reveals the Hsp90 client-remodelling mechanism. *Nature*, *601*(7893), Article 7893. https://doi.org/10.1038/s41586-021-04236-1

Pickett, C. L., Dietrich, N., Chen, J., Xiong, C., & Kornfeld, K. (2013). Mated progeny production is a biomarker of aging in *Caenorhabditis elegans*. *G3 Genes|Genomes|Genetics*, *3*(12), 2219–2232. https://doi.org/10.1534/g3.113.008664

Podshivalova, K., Kerr, R. A., & Kenyon, C. (2017). How a mutation that slows aging can also disproportionately extend end-of-life decrepitude. *Cell Reports*, *19*(3), 441–450. https://doi.org/10.1016/j.celrep.2017.03.062

Putker, M., Madl, T., Vos, H. R., de Ruiter, H., Visscher, M., van den Berg, M. C. W., Kaplan, M., Korswagen, H. C., Boelens, R., Vermeulen, M., Burgering, B. M. T., & Dansen, T. B. (2013). Redox-dependent control of FOXO/DAF-16 by transportin-1. *Molecular Cell*, *49*(4), 730–742. https://doi.org/10.1016/j.molcel.2012.12.014

Ratnappan, R., Amrit, F. R. G., Chen, S.-W., Gill, H., Holden, K., Ward, J., Yamamoto, K. R., Olsen, C. P., & Ghazi, A. (2014). Germline signals deploy NHR-49 to modulate fatty-acid β-oxidation and desaturation in somatic tissues of *C. elegans*. *PLoS Genetics*, *10*(12), e1004829. https://doi.org/10.1371/journal.pgen.1004829

Rottiers, V., Motola, D. L., Gerisch, B., Cummins, C. L., Nishiwaki, K., Mangelsdorf, D. J., & Antebi, A. (2006). Hormonal control of *C. elegans* dauer formation and life span by a Rieske-like oxygenase. *Developmental Cell*, *10*(4), 473–482. https://doi.org/10.1016/j.devcel.2006.02.008

Schaar, C. E., Dues, D. J., Spielbauer, K. K., Machiela, E., Cooper, J. F., Senchuk, M., Hekimi, S., & Van Raamsdonk, J. M. (2015). Mitochondrial and cytoplasmic ROS have opposing effects on lifespan. *PLoS Genetics*, *11*(2), e1004972. https://doi.org/10.1371/journal.pgen.1004972

Schiffer, J. A., Stumbur, S. V., Seyedolmohadesin, M., Xu, Y., Serkin, W. T., McGowan, N. G., Banjo, O., Torkashvand, M., Lin, A., Hosea, C. N., Assié, A., Samuel, B. S., O'Donnell, M. P., Venkatachalam, V., & Apfeld, J. (2021). Modulation of sensory perception by hydrogen peroxide enables *Caenorhabditis elegans* to find a niche that provides both food and protection from hydrogen peroxide. *PLOS Pathogens*, *17*(12), e1010112. https://doi.org/10.1371/journal.ppat.1010112

Senchuk, M., Dues, D., & Van Raamsdonk, J. (2017). Measuring oxidative stress in *Caenorhabditis elegans:* Paraquat and Juglone Sensitivity Assays. *BIO-PROTOCOL*, *7*(1). https://doi.org/10.21769/BioProtoc.2086

Shen, Y., Wollam, J., Magner, D., Karalay, O., & Antebi, A. (2012). A steroid receptor–microRNA switch regulates life span in response to signals from the gonad. *Science*, *338*(6113), 1472–1476. https://doi.org/10.1126/science.1228967

Son, H. G., Altintas, O., Kim, E. J. E., Kwon, S., & Lee, S.-J. V. (2019). Age-dependent changes and biomarkers of aging in *Caenorhabditis elegans*. *Aging Cell*, *18*(2), e12853. https://doi.org/10.1111/acel.12853

Stiernagle, T. (2006). Maintenance of *C. elegans. WormBook: The online review of C. elegans biology*, 1–11. https://doi.org/10.1895/wormbook.1.101.1

Sun, X., Chen, W.-D., & Wang, Y.-D. (2017). DAF-16/FOXO transcription factor in aging and longevity. *Frontiers in Pharmacology*, *8*. https://www.frontiersin.org/journals/pharmacology/articles/10.3389/fphar.2017.00548

Tatum, M. C., Ooi, F. K., Chikka, M. R., Chauve, L., Martinez-Velazquez, L. A., Steinbusch, H. W. M., Morimoto, R. I., & Prahlad, V. (2015). Neuronal serotonin release triggers the heat shock response in *C. elegans* in the absence of temperature increase. *Current Biology*, *25*(2), 163–174. https://doi.org/10.1016/j.cub.2014.11.040

Tiku, V., Jain, C., Raz, Y., Nakamura, S., Heestand, B., Liu, W., Späth, M., Suchiman, H. Eka. D., Müller, R.-U., Slagboom, P. E., Partridge, L., & Antebi, A. (2017). Small nucleoli are a cellular hallmark of longevity. *Nature Communications*, *8*, 16083. https://doi.org/10.1038/ncomms16083

Timmons, L., Court, D. L., & Fire, A. (2001). Ingestion of bacterially expressed dsRNAs can produce specific and potent genetic interference in *Caenorhabditis elegans. Gene*, *263*(1–2), 103–112. https://doi.org/10.1016/s0378-1119(00)00579-5

Ward, S., & Carrel, J. S. (1979). Fertilization and sperm competition in the nematode *Caenorhabditis elegans*. *Developmental Biology*, *73*(2), 304–321. https://doi.org/10.1016/0012-1606(79)90069-1

Zhang, B., Xiao, R., Ronan, E. A., He, Y., Hsu, A.-L., Liu, J., & Xu, X. Z. S. (2015). Environmental temperature differentially modulates *C. elegans* longevity through a thermosensitive TRP channel. *Cell Reports*, *11*(9), 1414–1424. https://doi.org/10.1016/j.celrep.2015.04.066

Zhang, S., Li, F., Zhou, T., Wang, G., & Li, Z. (2020). *Caenorhabditis elegans* as a useful model for studying aging mutations. *Frontiers in Endocrinology*, *11*. https://doi.org/10.3389/fendo.2020.554994

Biography

Margareta Sačer (born on 12th of July 1999 in Zagreb, Croatia), after finishing high school education at the V. gymnasium, started her academic journey as a bachelor student of molecular biology at the University of Zagreb in 2018. In 2021, she obtained a bachelor's degree with a thesis on *Serotonin as a signalling molecule in peripheral tissues* under the supervision of Dubravka Hranilović. Margareta pursued her master's in molecular biology at the University of Zagreb starting in October 2021. Throughout her studies, she acquired research experience in lizard behaviour and molecular tests at the faculty's Department of Animal Physiology. She also worked as a laboratory practice demonstrator, aiding students in practical Molecular Biology of the Cell classes. In the summer of 2022, she received the Summer Scholarship from the IOCB Prague which enabled her to research neuroprotective properties of anorexigenic peptides in Lenka Maletínská group. That year she also did an internship at the Neurochemistry and Molecular Neurobiology Laboratory at the Ruđer Bošković Institute in Jasminka Štefulj group where she researched placental serotonin. In 2023, after obtaining the Erasmus+ Internship Scholarship, she did the experimental work for her master's thesis in the Antebi laboratory at the Max Planck Institute for Biology of Ageing in Cologne.

Margareta enjoys science popularisation activities as well. Apart from being an active member of student Neurobiology and Microbiology Groups where she regularly held lectures, she published an article titled "Microbiome and Mental Health" in the students' magazine "In Vivo". As a co-founder of a youth PROMISE association of students in biomedical fields that focuses on the popularisation of science and postulates of personalised medicine, she was one of the organisers of the international Brain-Gut Axis student conference, sponsored by the Croatian President. For this work, she was awarded the University of Zagreb Rectors´ Award for socially beneficial work in the academic and broader community.

Additionally, in her free time, she enjoys music-related activities, having studied classical singing and violin at Music School Vatroslav Lisinski and Music School Pavao Markovac.

Supplementary

Supplementary Table 1. DAF-16::GFP localisation at 25 ℃ in daf-16::gfp (luciferase and daf-41i), daf-16::gfp;glp-1 (luciferase and daf-41i), daf-16::gfp;glp-1ncl-1 (luciferase and daf-41i), daf-16::gfp daf-16i and daf-16::gfp daf-2i worms. The table contains the number of worms per biological replicate with no nuclear signal, weak, medium or strong nuclear signal. I calculated the ratio of this number and the total number of worms.

	Strain	*daf-16::gfp*				*daf-16::gfp daf-41i*			*daf-16::gfp;glp-1*		*daf-16::gfp;glp-1 daf-41i*	*daf-16::gfp;glp-1ncl-1*		*daf-16::gfp;glp-1ncl-1 daf-41i*		*daf-16::gfp daf-16i*	*daf-16::gfp daf-2i*
	Biological replicate	1	2	3	4	1	2	3	1	2	1	1	2	1	2	1	1
N (worms)	No signal															7	
	Weak	2	1						2			3					
	Medium	10	1	7	9		5	10	7			4	8	1			
	Strong	1	8	2	3	9	9	1	1	10	10	3		12	9		9
	Total	13	10	9	12	9	14	11	10	10	10	10	8	13	9	7	9
Ratio	No signal	0	0	0	0	0	0	0	0,00	0,00	0,00	0,00	0,00	0,00	0,00	1,00	0,00
	Weak	0.15	0.1	0	0	0	0	0	0,20	0,00	0,00	0,30	0,00	0,00	0,00	0,00	0,00
	Medium	0.77	0.1	0.78	0.75	0	0.36	0.91	0,70	0,00	0,00	0,40	1,00	0,08	0,00	0,00	0,00
	Strong	0.08	0.8	0.22	0.25	1	0.64	0.09	0,10	1,00	1,00	0,30	0,00	0,92	1,00	0,00	1,00
Cytosolic	No signal	0	0	0	0	0	0	0	0,00	0,00	0,00	0,00	0,00	0,00	0,00	0,00	0,00
Cytosolic + nuclear	Weak + medium	0.92	0.2	0.78	0.75	0	0.36	0.91	0,90	0,00	0,00	0,70	1,00	0,08	0,00	0,00	0,00
Nuclear	Strong	0.08	0.8	0.22	0.25	1	0.64	0.09	0,10	1,00	1,00	0,30	0,00	0,92	1,00	0,00	1,00

Supplementary Table 2. HSF-1 nuclear foci formation in hsf-1::gfp, hsf-1::gfp daf-41i and hsf-1::gfp hsf-1i worms at 25 ℃ and after 30-min 37 ℃ exposure. Each BR (biological replicate) had 7 to 10 worms. For each worm a number of HSF-1 positive foci hypodermal tail cells was counted and divided by the total observed number to calculate the ratio.

25 ℃							*37 ℃*						
hsf-1::gfp	1 BR			2 BR			*hsf-1::gfp*	1 BR			2 BR		
worm	N foci	N total	ratio	N foci	N total	ratio	worm	N foci	N total	ratio	N foci	N total	ratio

1	10	17	0.59	0	17	0	1	7	8	0.88	13	17	0.76
2	3	17	0.18	6	17	0.35	2	16	17	0.94	15	17	0.88
3	5	17	0.29	0	17	0	3	17	17	1	8	17	0.47
4	8	17	0.47	9	17	0.53	4	17	17	1	12	17	0.71
5	6	17	0.35	0	17	0	5	17	17	1	9	17	0.53
6	2	17	0.12	0	17	0	6	16	17	0.94	17	17	1
7	3	14	0.21	0	17	0	7	17	17	1	10	17	0.59
8	5	16	0.31	0	17	0	8				12	17	0.71
9	6	16	0.38				9				8	17	0.47
											10	17	0.59

hsf-1::gfp daf-41i							*hsf-1::gfp daf-41i*						
1	9	17	0.53	9	17	0.53	1	17	17	1	0	17	0
2	8	17	0.47	17	17	1	2	7	7	1	12	17	0.71
3	9	17	0.53	9	17	0.53	3	10	10	1	9	17	0.53
4	12	17	0.71	11	17	0.65	4	3	3	1	7	17	0.41
5	6	15	0.4	16	17	0.94	5	4	4	1	11	17	0.65
6	8	17	0.47	12	17	0.71	6	4	4	1	11	17	0.65
7	4	17	0.24	10	17	0.59	7	7	7	1	17	17	1
8	8	17	0.47	15	17	0.88	8	17	17	1	17	17	1
9	7	17	0.41	14	17	0.82	9	17	17	1			
10	6	17	0.35				10	17	17	1			

hsf-1::gfp hsf-1i							*hsf-1::gfp hsf-1i*						
1	0	18	0	2	17	0.12	1	1	17	0.06	0	17	0
2	2	19	0.11	0	17	0	2	1	17	0.06	0	17	0
3	5	20	0.25	0	17	0	3	2	17	0.12	1	17	0.06
4	4	21	0.19	0	17	0	4	5	17	0.29	1	17	0.06
5	6	22	0.27	0	17	0	5	3	17	0.18	0	17	0
6	10	23	0.43	0	17	0	6	4	17	0.24	4	17	0.24
7	6	24	0.25	0	17	0	7	1	17	0.06	3	17	0.18
8	4	25	0.16	1	17	0.06	8	2	17	0.12	2	17	0.12
9	6	26	0.23	3	17	0.18	9	0	17	0			
10	6	27	0.22				10	0	17	0			